Faculty of Medicine and Life Sciences
School for Life Sciences

Master of Biomedical Sciences

Master's thesis

Recovery capacity of highly regenerative organisms exposed to gamma radiation: comparison between the duckweed Lemna minor and planarian Schmidtea mediterranea

Joline Millen

Thesis presented in fulfillment of the requirements for the degree of Master of Biomedical Sciences, specialization

Environmental Health Sciences

SUPERVISOR :

Prof. dr. Karen SMEETS

SUPERVISOR :

Prof. dr. Nele HOREMANS

2020
2021

Faculty of Medicine and Life Sciences
School for Life Sciences

Master of Biomedical Sciences

Master's thesis

Recovery capacity of highly regenerative organisms exposed to gamma radiation: comparison between the duckweed Lemna minor and planarian Schmidtea mediterranea

Joline Millen
Thesis presented in fulfillment of the requirements for the degree of Master of Biomedical Sciences, specialization Environmental Health Sciences

SUPERVISOR :
Prof. dr. Karen SMEETS
SUPERVISOR :
Prof. dr. Nele HOREMANS

Recovery capacity of highly regenerative organisms exposed to gamma radiation: comparison between the duckweed *Lemna minor* and planarian *Schmidtea mediterranea* *

Joline Millen[1,2], Nele Horemans[1,3], Karen Smeets[2]

[1]Biosphere Impact Studies, SCK CEN, Boeretang 200, B-2400 Mol
[2]Zoology: Biodiversity and Toxicology, Centre for Environmental Research, Hasselt University, Campus Diepenbeek, Agoralaan Gebouw D, B-3590 Diepenbeek
[3]Environmental Biology, Centre for Environmental Research, Hasselt University, Campus Diepenbeek, Agoralaan Gebouw D, B-3590 Diepenbeek

*Running title: *Recovery capacity after exposure to γ-radiation*

To whom correspondence should be addressed: Prof. dr. Karen Smeets, Tel: +32 11 26 83 19; Email: karen.smeets@uhasselt.be

Keywords: apoptosis, DNA repair, gamma radiation, *Lemna minor*, mitosis, recovery capacity, *Schmidtea mediterranea*

ABSTRACT
    Gamma radiation can induce DNA damage in all organisms. However, highly regenerative organisms such as the duckweed *Lemna minor* and the planarian *Schmidtea mediterranea*, have high developmental plasticity because of their meristem and stem cells respectively, thereby enabling recovery. To determine the cellular mechanisms underlying recovery in these organisms exposed to genotoxic gamma radiation, DNA repair activity, and levels of mitosis and apoptosis were studied. Both organisms were exposed to gamma radiation for one week, followed by a seven-day recovery with sampling at day 0, 3 and 7. The applied dose rates were 68, 116 and 153 mGy/h for duckweed and 18, 29 and 83 mGy/h for planarians. First, the recovery capacity was determined by evaluating growth characteristics of duckweed and amputated planarians. Subsequently, DNA repair activity and apoptosis were analyzed at the transcriptional level via qPCR. The mitotic activity of the planarian stem cells was measured via anti-phospho-histone H3 immunostaining. Growth analyses in both organisms showed that recovery initiated earlier for lower exposure levels. DNA repair and apoptosis levels both increased before the recovery initiated in *L. minor*, while these analyses did not demonstrate a dose-dependent relation with the growth in *S. mediterranea*. However, before regeneration of the planarians was initiated, their mitotic activity increased. These results suggest that active DNA repair and apoptosis in *L. minor* and increased mitosis in *S. mediterranea* precede the onset of recovery. Further research will need to investigate the involved signaling pathways and their universality throughout species.

INTRODUCTION
    Ionizing radiation
Sources of ionizing radiation can be both natural and anthropogenic. All organisms are continuously exposed to low dose rates of radiation (1-4). Natural sources include cosmic radiation, radon, transuranic radionuclides and radioactive minerals in food products, air, water and soil. Additionally, organisms can be exposed to artificial radiation sources such as medical applications, industry, nuclear power production, research and nuclear accidents or attacks (1-4). In Belgium, the average exposure of the public to ionizing radiation is estimated at 5.1 mSv/year by the Federal Agency for Nuclear Control (FANC) in 2018 (5). Around 55% of this exposure was due to natural sources, the other 45% was almost completely caused by medical applications, with less than 0.2% from industrial applications (5).
Ionizing radiation includes every type of radiation that induces direct or indirect ionization with a subsequent energy transfer caused by an interaction

with matter. A radionuclide (RN) is an atom containing excess energy, *i.e.* an isotope with an unstable nucleus. The RN will release energy to transform into a more stable isotope. This process is called radioactive decay (6). An example of a RN is ^{137}Cs, derived from the element cesium (Cs), which has one stable isotope, ^{133}Cs (7).

Gamma (γ) radiation is an electromagnetic form of energy that is released when radioactive beta decay occurs in an element. During this transformation, residual energy is produced, which is stored in the daughter nucleus of the beta decay process. This residual energy is released during a second decay process in the form of photons, called gamma radiation, and depends on the type of RN (1, 8). These photons can interact with the electrons of atoms, thereby producing ionizing effects. This means that gamma radiation, *i.e.* the photons, are indirectly ionizing (1, 9). Additionally, the photons are uncharged, have no mass, move at the speed of light and have a high energy state (3, 10). These characteristics enable gamma radiation to travel faster, over longer distances and further through matter than other types of ionizing radiation, *i.e.* causing gamma radiation to have a higher penetrating power (1, 2). As a result, gamma radiation can affect organisms externally while the source can be relatively far away (2). The RN ^{137}Cs is a source of beta and gamma radiation and will be used in this study as the gamma source (7).

Genotoxicity of gamma radiation

Gamma radiation is mostly harmful to organisms when exposed from a distance due to its high penetrating power, inducing DNA damage in cells over the entire organism (11). It has been shown in both *in vivo* and *in vitro* studies of plants, prokaryotes, planarians, mammals and humans that gamma radiation induces genotoxic damage (2, 12). This DNA damage can be induced directly, causing double-strand breaks (DSBs), single-strand breaks (SSBs), base lesions or DNA-protein cross-linkages, where DSBs are the most dangerous type since the complementary fragment, used as a basis for the repair process, is missing (13-15). While indirect DNA damage is caused by reactive oxygen species (ROS), comprising both free radical and non-free radical oxygen intermediates, which at their turn interact with the DNA (1, 14, 16). The major genotoxic endpoints that can be observed after gamma irradiation include DSBs, chromosome breaks and aberrations, sister chromatid exchange, induction of micronuclei, reciprocal translocations, mutations, sperm abnormalities, DNA fragmentation and abnormal karyotypes (1, 2, 14).

However, cells can respond to induced damages by initiating DNA damage response (DDR) pathways and damage-bypass mechanisms. These enable the cells to, respectively, reverse or tolerate the damage to a certain extent, allowing the organisms to recover from the induced damage. There are at least five different DNA repair pathways that cells can activate depending on the type of damage and the cell cycle stage, including nucleotide excision repair (NER), base excision repair (BER), homologous recombination (HR), nonhomologous end-joining (NHEJ) and mismatch repair (MMR). HR and NHEJ are the two principal repair pathways for DSBs (13). Direct chemical reversal and interstrand crosslink (ICL) repair can remove a few specific lesions. Furthermore, translesion synthesis (TLS) is a well-known tolerance pathway, using specific polymerases to bypass the damage and continue replication (16). The proteins encoded by the genes *ku80, mre11, pold1, rad18, rad50, rad51* and *rev1* are involved in DSB repair by either NHEJ, HR or both (17-25). Additionally, the protein of *pold1* also functions in BER, NER and MMR (21). A second function of *rad18* and *rad51* is ICL repair (17, 19, 20, 24, 25). Furthermore, *pcna, pold1, rad18* and *rev1* are involved in TLS, and *pcna* also functions in NER (21, 22, 24, 26). The nomenclature for genes differs between organisms, however, to retain a uniform style throughout this text, all gene abbreviations are written in small italic letters. When the genes responsible for these mechanisms are damaged themselves or there is too much DNA damage, the above-described cellular mechanisms are not able to repair or bypass the damage, and apoptosis, tumor formation or necrotic cell death can be induced (13, 16). Apoptosis is a form of programmed cell death. It is a highly-regulated process used, among other functions, as a defense against DNA damage induced by genotoxic exposure such as gamma radiation (27). Therefore, it can be seen as an alternative to the DNA repair mechanisms (28). Bcl2 associated athanogene 4 (*bag4*) encodes for a BAG protein, a plant homolog for apoptotic-like regulation. It prevents the onset and presence of programmed cell death, *i.e.*

apoptosis (29). Caspase-3, encoded by *casp3*, plays a central role in the execution of cell apoptosis (30). Furthermore, the protein encoded by *bax* promotes apoptosis by activating, among others, Caspase-3, while the protein of *bcl2* functions anti-apoptotic by inhibiting caspase activation (31).

A previous study on human cells suggests that the genotoxic effect of gamma radiation is a combination of induced DNA damage and reduced DNA repair capacities (32). Therefore, the balance between DNA damage and repair/tolerance mechanisms is crucial for organisms to return to their normal state and resume growth after exposure to gamma radiation, and genotoxic stress in general. In this study, the ability to resume growth determines the recovery capacity of the organisms.

Lemna minor

Lemnaceae are a family of aquatic duckweed species with floating plant bodies, called "fronds" or "thalli", and reduced root structures, called "rhizoids" (33). Duckweeds are freshwater angiosperms, more specifically monocotyledon macrophytes. The common duckweed, *Lemna minor*, has a great ecological significance since this species is an important part of the first trophic level of the aquatic food chain (34). When conditions are favorable, *L. minor* can grow and asexually reproduce in different climates with extreme speed, producing genetically identical clones. A previous study described that *L. minor* exhibited a doubling time of 2.3 days in laboratory conditions using Hoagland medium (35). The vegetative propagules are produced by mitotic cell division in two lateral reproductive pouches in each frond. Inside a meristematic pouch of the mother frond, a primordial bud develops leading to a daughter frond. In time, the daughter frond detaches by breaking the stipe and becomes an independent colony (33, 36).

Lemnaceae have a high biomass production rate, making them interesting for several economical applications, including biofuel production (37, 38), feed source for animals (39, 40), wastewater treatment (41, 42), phytoremediation (43, 44) and pharmaceutical applications (45). Another application of *Lemna minor* is ecotoxicological research. Since its growth rate is very sensitive to environmental (biotic and abiotic) changes, this plant is often used as a model organism for toxicity testing in higher aquatic plants. Standardized guidelines to perform growth inhibition tests are described by the OECD, among others (46). Since this organism is often studied, our research group at SCK CEN analyzed and provided a first draft of the genome of *L. minor* (47).

Schmidtea mediterranea

Schmidtea mediterranea is a freshwater planarian, a free-living, unsegmented, bilaterally symmetric flatworm of the Tricladida order. They are found on islands and coastal areas of the Western Mediterranean with a temperate climate (48). *S. mediterranea* is a well-known model organism for regeneration, development, tissue homeostasis and stem cell research (49). It has a unique regeneration capacity as it can regenerate a fully functioning organism from a small body fragment in four to seven days (50). This plasticity is due to its large number of stem cells (25-30% of all cells), called neoblasts, maintained throughout its adult life (51). The neoblasts are the only proliferating cells present in the planarian and migrate to a wound site to form a blastema, which regenerates the missing body parts (52, 53). A controlled interplay between mitosis, differentiation of the neoblasts and apoptosis of differentiated cells is crucial for the remodeling process of the planarian, triggering recovery of the organism when well-balanced (31, 54). This controlled balance is also important for the planarian's response to the level of nutrient supply, causing acute growth or degrowth respectively with an abundance of food or starvation (55).

S. mediterranea has both a hermaphroditic sexual strain and an asexual strain reproducing by transverse fission, creating genetic clones (49). This planarian is often used as a model organism in (eco)toxicological studies because these strains are easily reproduced and handled in laboratory conditions, their neoblasts induce interesting processes as described above and their phylogenetic characteristics are unique (56-59). Since this organism is widely studied, adequate knowledge of its genome is available (60, 61).

Pluripotent stem cells

The meristem cells in the pouches of *Lemna minor* and the neoblasts of *Schmidtea mediterranea* are both pluripotent stem cells, which means they are undifferentiated and can differentiate into all cell types of the organism (33, 62, 63). These cells are

responsible for the high regenerative capacity of the organisms and can repair damaged body structures. However, it is generally known that rapidly dividing cells, *i.e.* stem cells, are more sensitive to radiation than non-dividing cells, which is a problem for the preservation of the genomic integrity and homeostasis of the organism (64, 65). To prevent these deleterious effects, the stem cells have developed an enhanced activity of highly efficient DNA repair compared to more differentiated cells, or they can activate apoptosis (65, 66). Furthermore, the sensitivity of the cells also depends on their phase in the cell cycle (67). During the cell cycle, checkpoint signaling controls whether the cell will mitotically divide, replicate the DNA, repair the DNA or activate apoptosis (Fig. 1) (68). When DNA errors are detected during the G1 phase of the cell cycle, a growth arrest can be observed, the cell will go into the G0 phase where proliferation is inhibited. However, this growth arrest is only temporary when the damage can be repaired, after which the mitotic cell division can proceed, enabling recovery from genotoxic exposure (28, 69). Although this process is proven to be true in numerous organisms, it is still under investigation for planarians. The proteins encoded by *atm, atr* and *h2ax* are involved in checkpoint signaling and cell cycle arrest in the presence of DNA damage (70).
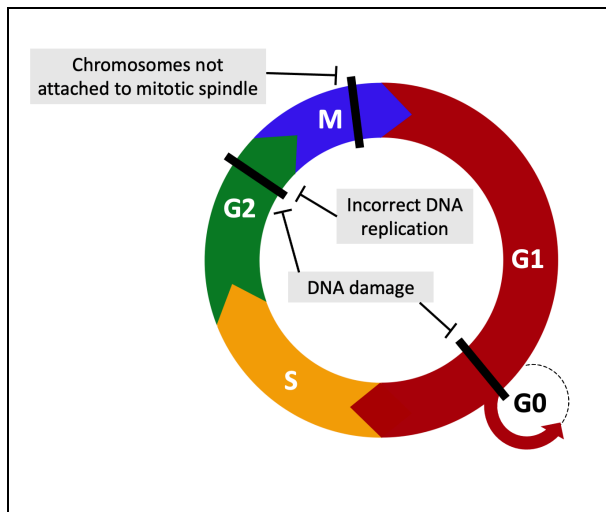

Fig. 1 – The checkpoints in the different phases of the cell division cycle. The checkpoints are marked with a black line and the grey boxes show causes for cell cycle interruption. G1: gap 1 phase (cell growth). S: synthesis phase (DNA replication). G2: gap 2 phase (cell growth). M: mitosis and cytokinesis phase (cell division). G0: cell cycle arrest phase.

Therefore, we hypothesize that the switch from growth inhibition to recovery in *Lemna minor* and *Schmidtea mediterranea* after exposure to gamma radiation depends on the level of induced DNA damage and the activity of the repair mechanisms. To test this hypothesis, first, the turning point between growth inhibition and induction was determined during a seven-day recovery period after a week of exposure to three different dose rates of gamma radiation per organism. Subsequently, cellular mechanisms possibly involved in the induction of recovery were analyzed. These mechanisms included DNA repair, apoptosis and mitosis.

EXPERIMENTAL PROCEDURES

Cultivation of the organisms

L. minor plants (serial number 1007 and ID number 5500) were cultured aseptically by adding three plants every 10-12 days in 250 mL Erlenmeyer flasks with 100 mL of 1/10 Hoagland medium (71). A pre-culture consisting of seven plants with three to four fronds per Erlenmeyer was started at 24°C for seven days with 14 hours of light per day from growth bulbs (LED) with an intensity of 110-120 µmol/s/m². At the start of the exposure experiment, five plants with three to four fronds were transferred to sterile 250 mL Nalgene® pots with 100 mL of the Hoagland solution. A sterilized floating ruler of 1 cm was added as a scale. The pots were covered with a transparent and sterile Petri dish, allowing light transmission.

An asexual strain of *S. mediterranea* was used for the experiments (72, 73). The planarians were cultured in the dark, at 20°C and in Milli-Q water supplemented with the following minerals: 0.1 mM KCl, 0.1 mM $MgCl_2$, 1.0 mM $MgSO_4$, 1.0 mM $CaCl_2$, 1.6 mM NaCl and 1.2 mM $NaHCO_3$. They were fed once a week with veal liver (59). Prior to the experiments, the planarians were starved for 11 days. During the exposure and recovery, the planaria were cultured in Petri dishes (d=3.5cm) containing 1 mL of the above-described medium per animal.

Experimental set-up of the organisms

Both organisms were chronically exposed for seven days to 3 different dose rates of gamma radiation in a radiation chamber with a horizontal ^{137}Cs source, at 20.6±1.5°C and with a 14/10h day/night cycle

4

with a light intensity of 110-120 µmol/s/m² provided by LED lights. The planarians were shielded from the light. The applied dose rates depended on the distance from the source (Table S1 in supplement). Common duckweed was exposed to dose rates of 68 (γ_{68}), 116 (γ_{116}) and 153 (γ_{153}) mGy/h of gamma radiation. The planarians were exposed to 18 (γ_{18}), 29 (γ_{29}) and 83 (γ_{83}) mGy/h. Controls (C) and recovering organisms were incubated in a separate climate chamber with the same temperature and light conditions. After 7 days of exposure, five *L. minor* plants with at least three fronds were transferred into a new sterile pot with fresh Hoagland medium for the regrowth. To induce regeneration in the planarians, they were amputated in front of the pharynx immediately after the radiation experiment, providing an anterior (head) and posterior (tail) piece per animal. To investigate the recovery of the organisms, samples for the different assays were taken immediately at the end of radiation (recovery day 0), and at day 3 and 7 of the recovery period. For all parameters, biological replicates were taken from multiple pots or Petri dishes.

Measurements of growth characteristics

Top-view pictures of the *L. minor* pots were made before and after the exposure and at day 0, 3 and 7 of the recovery. These pictures were analyzed with ImageJ (version 2.1.0) to measure the surface area of the fronds and count the number of fronds per pot. The fresh weight was determined as described by Van Hoeck *et al.*, 2015 (71). The obtained values of the total surface area, number of fronds and fresh weight were used to determine the average specific growth rate according to the OECD guidelines (46). Subsequently, the corresponding percentage inhibition in average specific growth rate (%GI) was calculated as described by these guidelines.

The heads and tails of ten amputated planaria were top-view photographed in triplicate per dose rate at day 0, 3 and 7 of recovery, using a Ceti Varizoom Binocular Stereo Microscope with Ceti Si-3000 camera (Medline Scientific, Oxon, UK). The images were analyzed using ImageJ (version 2.1.0), to determine growth activity based on the relative blastema area.

Transcriptional analysis

To measure the activity of DNA repair mechanisms and apoptosis levels at a transcriptional level, real-time qPCR for gene expression was performed. Detailed information of all the steps of the procedure and the included primers is summarized in Table S2 (*L. minor*) and S3 (*S. mediterranea*), based on the MIQE guidelines (74, 75).

For *S. mediterranea*, heads and tails were analyzed separately. RNA extractions of *L. minor* were performed with the RNeasy Plant Mini kit (QIAGEN, Hilden, Germany), according to the manufacturer's protocol. For the planarians, RNA extractions were performed using a phenol-chloroform extraction procedure as described by Pirotte *et al.*, 2015 (76). cDNA synthesis was executed using the TaKaRa PrimeScript RT Reagent kit (TaKaRa Bio Inc., Kusatsu, Shiga, Japan). The real-time qPCR measurements were performed with the Fast SYBR Green master mix (Applied Biosystems, Thermo Fisher Scientific, Foster City, CA, USA). The Rotor Gene Q platform (QIAGEN, Hilden, Germany) was used for the qPCR analysis of the plants and the QuantStudio 5 Real-Time PCR System, 384-well format (Applied Biosystems, Thermo Fisher Scientific, Foster City, CA, USA) for the planarians. Gene expression values were calculated relative to the normalization factor of the reference genes, following the $2^{-\Delta\Delta Ct}$ method (77).

Staining for mitotic index

To determine the mitotic index of the meristem cells of *L. minor*, tests with toluidine blue and Schiff's reagent stainings were performed. First, the samples were fixed, dehydrated and cleared, after which paraffin sections were made. Deparaffinization and rehydration were performed prior to the stainings. For stainings with toluidine blue, mounting with 50% glycerol and DPX were tested. The detailed protocol is described in Method S1 in supplement.

Anti-phospho-histone H3 (anti-H3P) antibody immunostaining

This assay was performed twice with six whole-mount planarians per condition to determine the mitotic activity of the neoblasts. The protocol was executed as described by Plusquin *et al.*, 2012 (78), with some small modifications, described here. The mucus layer was removed using 2% HCl in PBS. Animals were incubated in Carnoy's fixative for 2 hours at 4°C while shaking. Samples fixed at day 0 and 3 were kept in 100% methanol at -20°C until

the fixation of samples at day 7 was performed. Next, overnight bleaching was initiated for all samples. Blocking of the non-specific binding sites with 1% BSA in 0.3% PBST was performed for 2 hours. The primary antibody (rabbit anti-phospho-Histone H3; Invitrogen, Thermo Fisher Scientific, Waltham, Mass, USA) was diluted 1:1000 in 1% BSA/PBST. The planarians were washed 7 times with 0.3% PBST and incubated in BSA/PBST for 1 hour. Incubation in the secondary antibody (Alexa Fluor goat anti-rabbit 568), diluted 1:500 in BSA/PBST, was performed for 1 hour. The samples were mounted with Immu-Mount (Fisher Scientific, Thermo Fisher Scientific, Waltham, Mass, USA). Fluorescence microscopy analysis was executed with a Nikon Eclipse 80i microscope, equipped with a Nikon DS-Ri2 digital camera. The number of stained cells was determined relative to the total body area with ImageJ (version 2.1.0).

Alkaline comet assay

To detect DNA damage, the alkaline comet assay was performed for both organisms as described by Xie *et al*., 2019 with some modifications, as described in Method S2 in supplement (79). For *L. minor*, the assay was performed in the dark with one red lamp as the only light source in the room, eliminating photochemical reactions. The comets were visualized with the Nikon Eclipse 80i fluorescence microscope, equipped with a Nikon DS-Ri2 digital camera.

Statistical analysis

The Shapiro-Wilk test was performed to check for normality and the Levene's test to check the homogeneity of variance. When the assumptions were met, the results of the different dose rates and time points in recovery were compared by performing one-way and two-way ANOVA statistical analyses, followed by a Tukey HSD posthoc test with Benjamini-Hochberg FDR correction for multiple testing. When assumptions were not met, the results were transformed (log, square root, $1/x$ and e^x) before performing the analyses. When the assumptions were not met after transformation, the non-parametric Kruskal-Wallis test with Dunn's posthoc test was executed. The statistical analyses were performed with RStudio 1.2.5033 software (Boston, MA, USA), results were graphically displayed using GraphPad Prism vers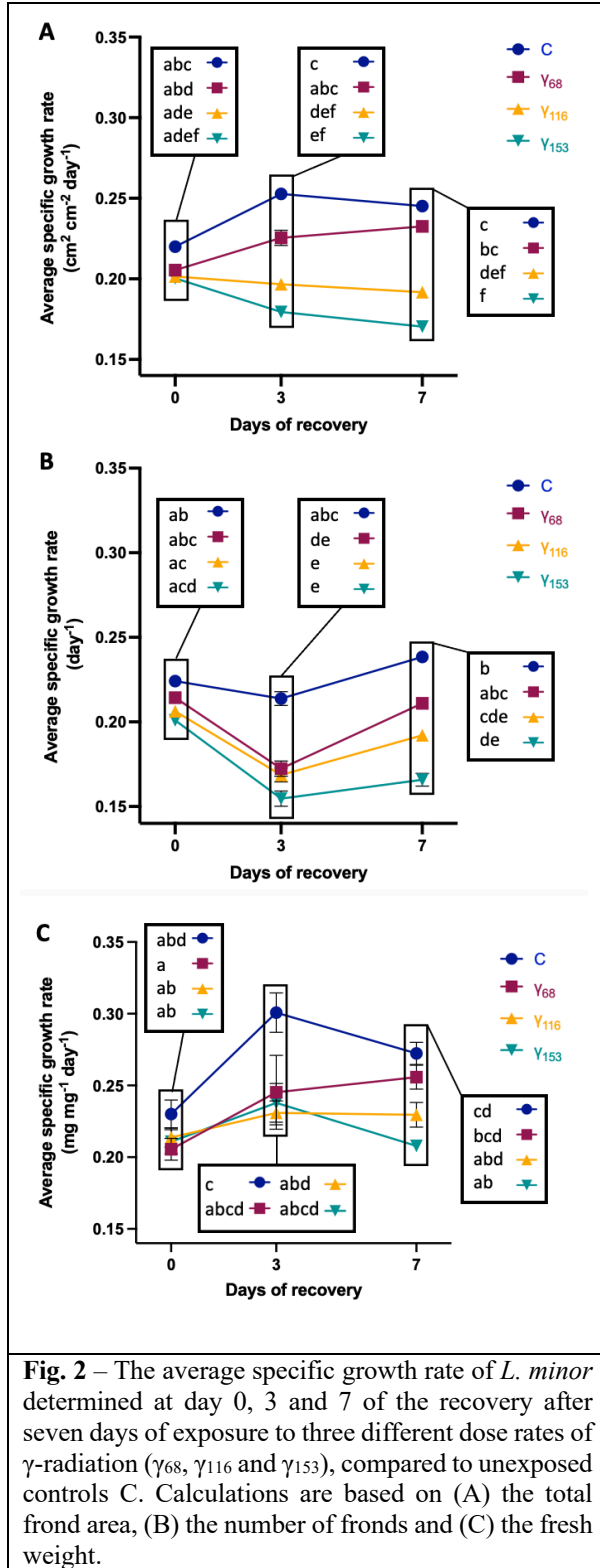ion 9.1.0 (San Diego, CA, USA). All data are presented as mean values ± standard error (SE) and p-values < 0.05 were considered significant.

RESULTS
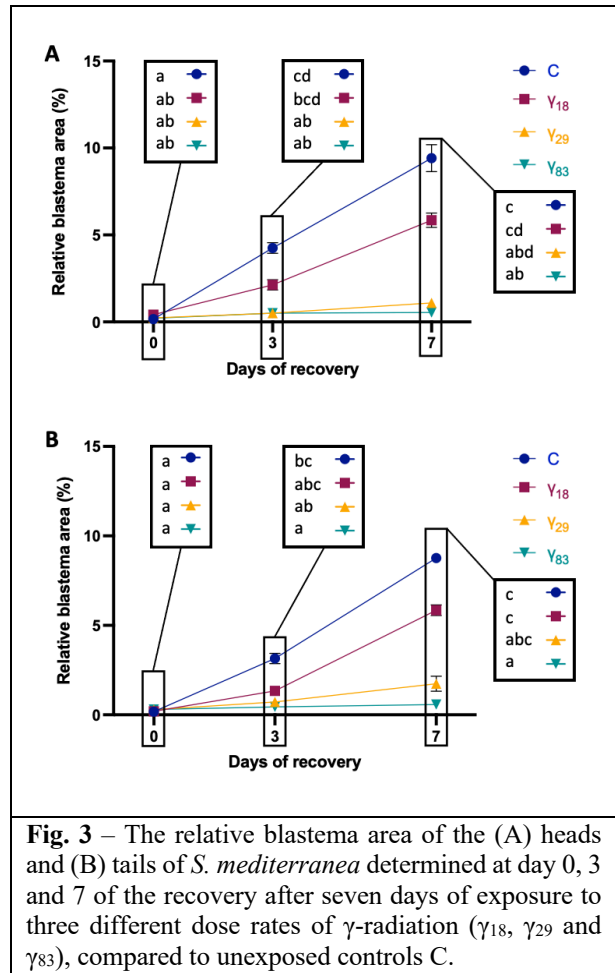
Growth characteristics

The average specific growth rate of *L. minor* during recovery was calculated based on the total frond area, number of fronds and fresh weight as shown in Fig. 2. These results were based on the analysis of at least 12 independent replicates for the total area and frond number and at least 6 replicates for fresh weight. All three endpoints showed that the average specific growth rate during recovery is lower when the dose rates of gamma radiation are higher. However, whether there was an increase, decrease or stagnation during the recovery period differed between the three endpoints. The total frond area demonstrated a higher growth rate for the control and lowest dose rate compared to the two highest dose rates during recovery, with no significant difference between γ_{68} and the control. Based on the number of *Lemna* fronds, all three dose rates showed a decrease in the growth rate at day 3 of the recovery. However, the values increased again for γ_{68} on day 7. The average growth rate based on the fresh weight of the plants increased over the total recovery period for the lowest dose rate, while γ_{116} and γ_{153} exhibited a stable growth. The percentage inhibition in average specific growth rate (%GI), calculated according to the OECD guidelines (46), displays these results relative to the control (0% GI), as shown in Fig. S1 in supplement. The %GI results of the fresh weight indicated that at day 7 of the recovery, the growth of γ_{68} and γ_{116} was not inhibited, which was also observed for the total frond area after exposure to the lowest dose rate.

The relative blastema area of *S. mediterranea* is the area responsible for the regeneration at the wound site relative to the total body area. It is a measure for the growth activity of the planarians and was analyzed for both the anterior (heads) and posterior (tails) pieces of the planarians, as shown in Fig. 3. The analysis was performed using the mean value of 10 biological replicates per condition. Analysis of both the heads and tails showed similar trends; animals exposed to the lowest dose rate (γ_{18}) demonstrated a clear growth over the seven days of recovery, while there was no growth after exposure to the two highest dose rates. However, a slight

6

Fig. 2 – The average specific growth rate of *L. minor* determined at day 0, 3 and 7 of the recovery after seven days of exposure to three different dose rates of γ-radiation (γ_{68}, γ_{116} and γ_{153}), compared to unexposed controls C. Calculations are based on (A) the total frond area, (B) the number of fronds and (C) the fresh weight.

heads during recovery from exposure to the lowest dose rate and their controls were slightly higher than these values of the tails.

Fig. 3 – The relative blastema area of the (A) heads and (B) tails of *S. mediterranea* determined at day 0, 3 and 7 of the recovery after seven days of exposure to three different dose rates of γ-radiation (γ_{18}, γ_{29} and γ_{83}), compared to unexposed controls C.

increase in relative blastema area was observed for tails exposed to γ_{29} between day 3 and 7 of the recovery. The relative blastema area values of the

Transcriptional analysis
To measure the activity of DNA repair mechanisms and apoptosis levels after the radiation exposure, gene expression levels of genes involved in these mechanisms were determined using qPCR. The results are based on qPCR analyses of six biological replicates of *L. minor* and 4-6 replicates of the tails of *S. mediterranea*. However, for γ_{29} and γ_{83} exposure of the planarian heads, there were time points during the recovery for which only one sample was fit for qPCR measurement. Therefore, only the results of the control and γ_{18} analyses, based on 3-6 replicates, were analyzed (Fig. S2).

1. DNA repair activity
Relative gene expression levels for genes involved in DNA repair mechanisms of *L. minor* are shown

in Fig. 4A-J. Control plants and plants exposed to γ_{68} were never significantly different and indicated an upregulation or a stagnation in relative gene expression of most DNA repair genes between day 0 and 3 of the recovery, followed by a decrease between day 3 and 7, whether or not significant. In contrast, the relative gene expression levels of exposure to γ_{153} and γ_{116} were mostly at a lower, constant level during the recovery period. The highest dose rate was significantly downregulated at day 3 of the recovery for *atm, atr, pold1* and *rad50* and at day 7 for *rev1* compared to the
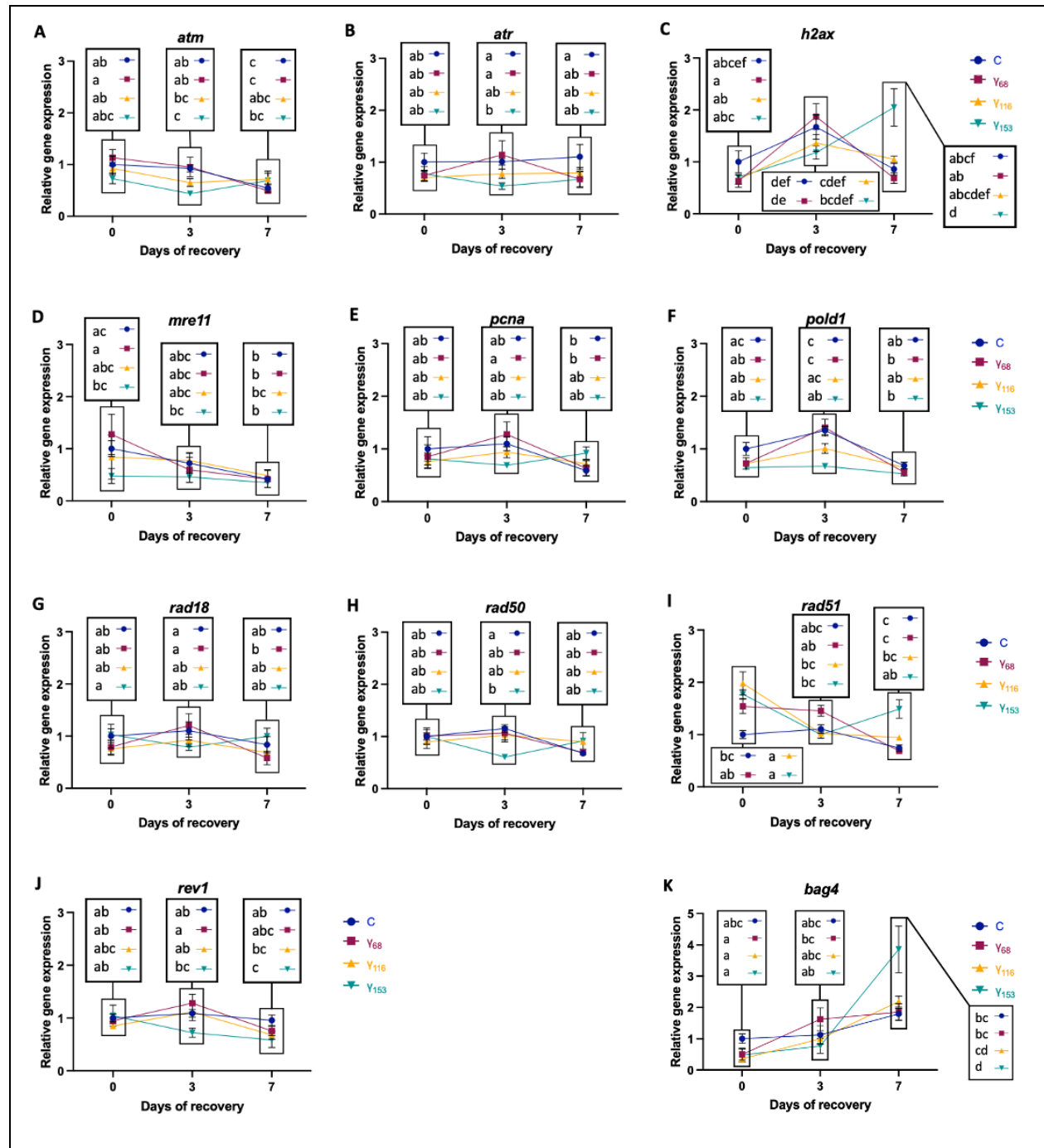

Fig. 4 – Relative gene expression levels of *L. minor* determined at day 0, 3 and 7 of the recovery after seven days of exposure to three different dose rates of γ-radiation (γ_{68}, γ_{116} and γ_{153}), compared to unexposed controls C. The genes are involved in (A-J) DNA repair pathways and (K) apoptotic regulation.

controls. A few genes, however, showed different patterns; the gene expression levels of *h2ax* after exposure to γ_{116} increased in the first three days of recovery, after which it stagnated, and exposure to γ_{153} initiated a constant increase in expression of the *h2ax* gene during recovery. The relative gene expression of *mre11* decreased for the control and lowest dose rate during the seven days of recovery.

The gene *rad51* demonstrated an upregulation of expression levels for all three dose rates at day 0 of the recovery period, which decreased at day 3 for γ_{153} and γ_{116} and stagnated between day 3 and 7 with a slight increase for γ_{153}. In contrast, *rad51* expression stagnated between day 0 and 3 of the recovery for γ_{68} after which it decreased between day 3 and 7.
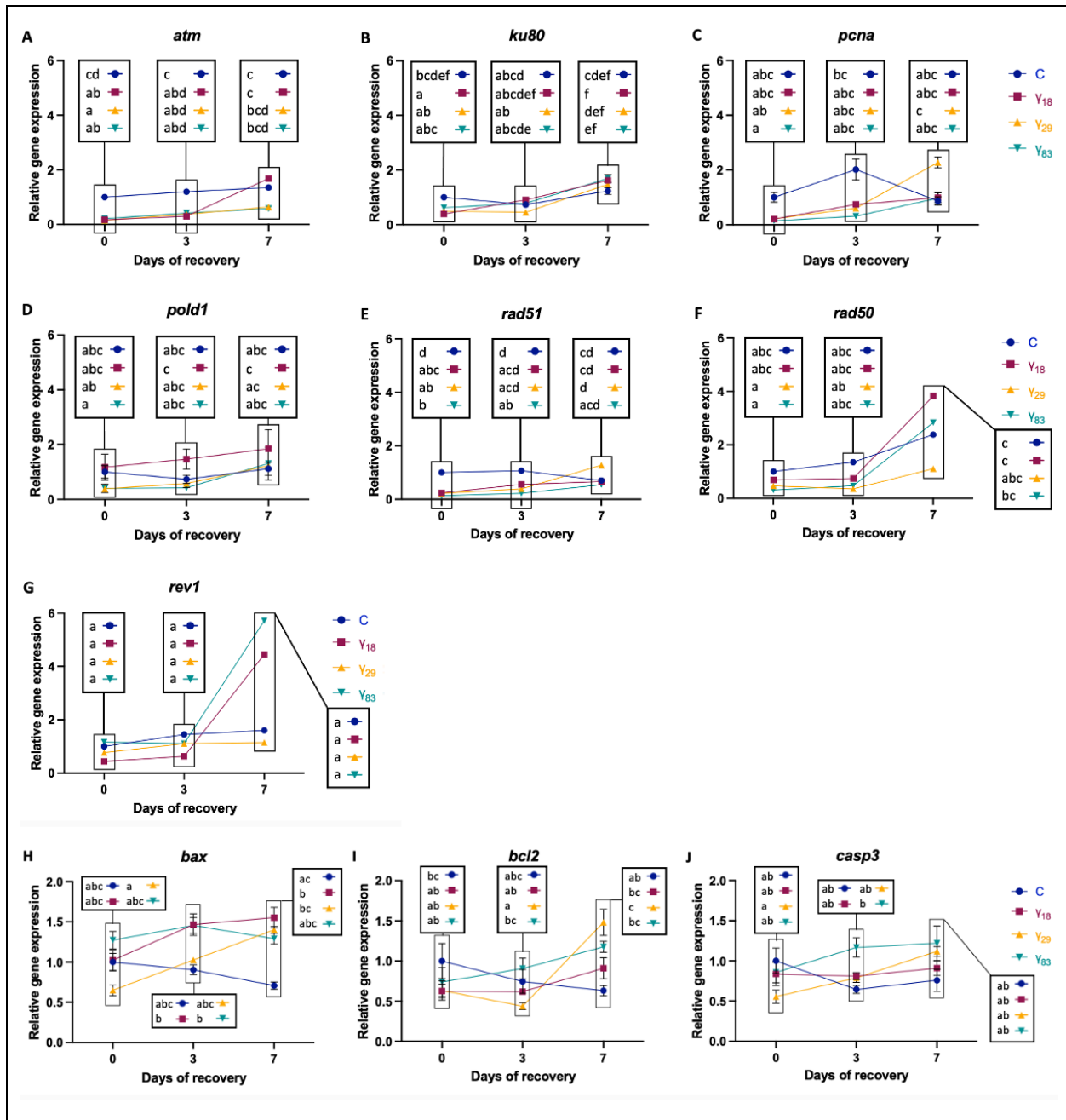

Fig. 5 – Relative gene expression levels of the tails of *S. mediterranea* determined at day 0, 3 and 7 of the recovery after seven days of exposure to three different dose rates of γ-radiation (γ_{18}, γ_{29} and γ_{83}), compared to unexposed controls C. The genes are involved in (A-G) DNA repair pathways and (H-J) apoptotic regulation.

The relative gene expression levels of the tails of exposed planarians, presented in Fig. 5A-G, demonstrated either a stagnation or an upregulation of all DNA repair genes during the recovery period. At day 0 of the recovery, all gene expression levels were either at similar levels as the control or downregulated, which was significant for all dose rates in *atm* and *rad51*, and for *ku80* expression after γ_{18} exposure. Furthermore, the transcription levels of all measured genes remained stable between day 0 and 3 of the recovery. Between day 3 and 7, there was an upregulation of *atm* for γ_{18}. Over the seven days of recovery, the gene expression of *pcna* increased for tails exposed to γ_{29}, *rad50* was upregulated for γ_{18} and γ_{83}, and *rad51* expression increased for γ_{29}. The expression levels during the recovery of the planarian heads exposed to γ_{18} and the corresponding controls showed similar trends of stagnation and increase, however, the differences were never significant (Fig. S2A-G).

2. Apoptotic activity

To analyze the apoptotic cell activity of exposed *L. minor* plants, the relative gene expression of *bag4* was measured (Fig. 4K). For the lowest dose rate (γ_{68}), the *bag4* expression was upregulated between day 0 and 3 of the recovery, after which it stagnated. *L. minor* plants exposed to a dose rate of 116 mGy/h showed a constant increase in *bag4* expression during the seven days of recovery. Furthermore, the *bag4* expression levels increased later in the recovery for the highest dose rate, between day 3 and 7, with a significant upregulation compared to the control levels.

For *S. mediterranea*, the relative expression levels of *bax*, *bcl2* and *casp3*, three genes involved in apoptotic regulation, were determined during the recovery period. After one week of recovery, all three genes showed higher expression levels of all exposed samples compared to the control, however, these differences were only significant for *bax* after γ_{18} exposure and *bcl2* after γ_{29} exposure. Transcription of the *bax* gene increased constantly during the seven days of recovery for samples exposed to γ_{29}. Additionally, an increase in *bcl2* expression was observed for γ_{29} between day 3 and 7 of the recovery. All other gene expression measurements of these three genes during the recovery showed stagnation with sometimes a slight increase for the exposed animals and a slight

decrease over time for the control, although none of these observations were significant. The expression levels of the planarian heads during recovery after exposure to γ_{18} and their corresponding controls showed similar trends, with no significant differences except an upregulation for γ_{18} exposure in the gene expression of *bax* at day 7 (Fig. S2H-J).

Mitotic activity

The toluidine blue and Schiff's reagent stainings were executed on *L. minor* sections to evaluate the mitotic index of the meristem cells. The plant tissues were successfully stained, however, mounting methods in combination with these stainings are still under optimization. Additionally, light microscopic analysis with a total magnification of 1000x was not sufficient to visualize the mitotic phases of the meristematic cells of *L. minor*, indicating that other microscopic and/or staining options should be considered in the future.

The phosphorylation of histone H3 plays an important role in cell division, making it a frequently used marker for mitotic cells. During the recovery of *S. mediterranea*, the proliferation of the neoblasts was measured based on the number of anti-H3P stained cells relative to the total body area (Fig. 6). The results were analyzed using the mean of at least five biological replicates per condition for the tails and at least three replicates for the heads. At the beginning of the recovery period, the number of dividing cells increased with lower exposure levels; however, these differences were not present anymore at day 7. For the controls and tails exposed to the two lowest dose rates, an increase in the number of mitotic cells was observed during the first three days of the recovery, which stagnated between day 3 and 7. Whereas during the total recovery period, a constant increase at a lower rate was observed for γ_{83}. Analysis of the mitotic levels of the heads showed one difference compared to the tails; there was an increase between day 3 and 7 of the recovery for animals exposed to γ_{29}.

Levels of DNA damage

The alkaline comet assay was performed to analyze the levels of DNA damage induced by gamma radiation in both organisms. However, visualization of stained nuclei of the controls, plants exposed to γ_{153} and planarians exposed to γ_{83}, indicated that
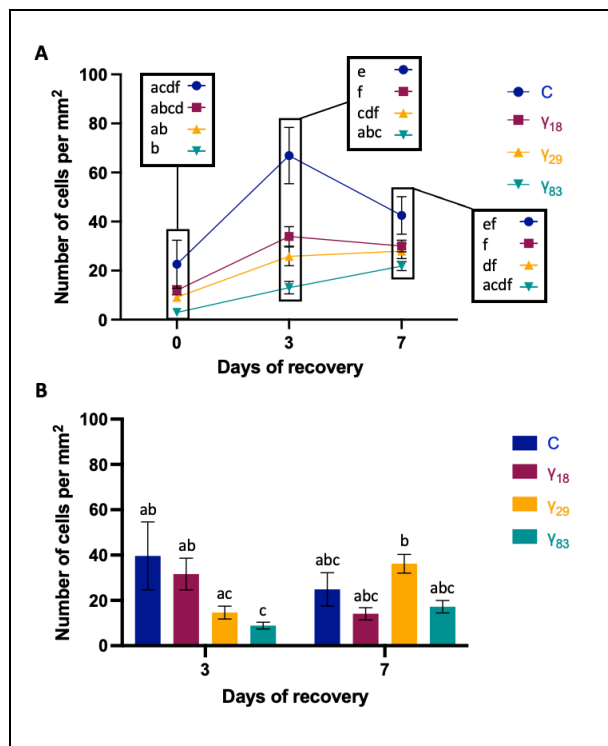
Fig. 6 – The number of mitotic neoblasts per mm^2 of the (A) tails and (B) heads of *S. mediterranea* during seven days of recovery after a week of exposure to three different dose rates of γ-radiation ($γ_{18}$, $γ_{29}$ and $γ_{83}$), compared to unexposed controls C. The mitotic levels were analyzed at day 0, 3 and 7 of the recovery for the tails. The analysis for the heads was only performed for day 3 and 7 of the recovery since values of the control at day 0 were missing.

there were no clear-cut differences in the length of the comet tails between the exposed and unexposed organisms at day 0 and 7 of the recovery (Fig. S3 for *L. minor*, Fig. S4 for *S. mediterranea*). Additionally, there were practical issues with the gels, causing a lot of samples to lose (most of) their nuclei, and a lot of background noise was detected for the assay executed with *L. minor*. All these factors together indicated that the protocol should be further optimized for both organisms before performing the analyses.

DISCUSSION

As stated above, gamma radiation can induce DNA damage, which leads to cell cycle arrest (11, 68, 69). When this arrest is induced in a large number of cells, general proliferation activity will decrease and growth inhibition may occur in the exposed organisms (80). In this study, the growth

responses during a week of recovery after exposure to high doses of gamma radiation were examined in *L. minor* and *S. mediterranea*.

The growth analyses during the recovery period of *L. minor* indicated that their recovery capacity depends on the exposure levels; growth is more inhibited after exposure to higher dose rates of chronic gamma radiation, which supports previous findings (71, 79, 80). However, the growth rates remained stable or increased over the total recovery period (Fig. 2), which demonstrates that *L. minor* tolerated all exposure conditions, confirming the results of Van Hoeck *et al*., 2017 (80). Plants exposed to the lowest dose rate ($γ_{68}$) are in recovery as indicated by the resumed increase in the growth rate during the total recovery period and the lack of significant differences between plants exposed to the lowest dose rate ($γ_{68}$) and control plants. The growth of the higher tested gamma exposures ($γ_{116}$ and $γ_{153}$) was inhibited during the seven days of recovery (Fig. S1). However, based on previous studies, it is expected that with a longer recovery period, the growth rate of these plants will increase again, thus, exhibiting recovery (80). These assumptions are also implied by the decreased growth inhibition for the fresh weight at day 7 of the recovery period after $γ_{116}$ exposure.

The recovery capacity of the planarians, determined based on the relative blastema area, was also dose-dependent. These findings correspond with the observed dose-dependency of growth in other organisms and the known genotoxic effect of gamma radiation possibly inducing a cell cycle arrest (28, 71, 79, 80). The increase in blastema area observed during the seven days of the recovery period for animals exposed to the lowest dose rate ($γ_{18}$) demonstrates that their recovery was initiated (Fig. 3). Planarians exposed to the two highest dose rates were still in growth arrest at the end of the seven-day recovery period. However, the slight increase in growth for $γ_{29}$ on the seventh day of the recovery indicates that the animals may be able to recover after a longer recovery period. This corresponds with the conclusions of a study on the effect of UV radiation in planaria, indicating that the radiation delayed planarian regeneration (81). Additionally, these results support the findings of Stevens *et al*., 2018, who stated that the neoblasts of *Schmidtea mediterranea* were able to recover from induced DNA damage after a three-day exposure to methyl methane-sulfonate (MMS;

50μM), thereby enabling successful regeneration of the planarians after genotoxic exposure (82). The slightly higher values for the relative blastema area of the heads compared to the tails might be explained by the fact that tails have a more difficult regrowth after genotoxic exposure, as described by Wouters *et al*., 2020 (83).

The growth capacity, and thus recovery, is for both *L. minor* and *S. mediterranea* dependent on the successful division of their meristem cells and neoblasts, respectively (33, 36, 52). This process of cell division is called mitosis.
As stated above, the activity in mitotic cell division could not be measured in *L. minor*. Therefore, an analysis of the effects of gamma radiation exposure on mitosis of the meristem cells during recovery was not included in this study.
The mitotic activity measurements in the tails of *S. mediterranea* showed a dose-dependent effect during the recovery period (Fig. 6). The increases in mitotic activity were higher for lower exposure levels during the first three days of the recovery, followed by stagnation. Whereas the mitotic activity for higher dose rates increased at a lower constant rate during the total recovery period. These findings demonstrate that the mitotic activity of the stem cells mostly increased when the recovery still needed to be induced and that once the animals were actively recovering from the induced stress, the mitotic activity stagnated. This outcome corresponds with previous studies that demonstrated the importance of mitosis of the neoblasts in the regeneration process of planarians after amputation (52, 53). Additionally, a dose rate-dependent effect of gamma radiation on mitotic activity was also observed in other freshwater planarian species (12).

Furthermore, the cell cycle has signaling checkpoints to detect DNA damage. When the DNA damage is discovered, the cells go into cell cycle arrest to enable DNA repair. When the damage is repaired, the cycle will be resumed (68). Therefore, DNA repair activity affects the levels of mitosis and can, thereby, influence growth (28, 69, 70).
For *L. minor* in control conditions or exposed to the lowest dose rate, the gene expression levels of all tested DNA repair genes followed similar trends during the seven days of recovery, which suggests

that the functioning of DNA repair mechanisms was not significantly affected by exposure to γ_{68} (Fig. 4A-J). In contrast, for the highest dose rate tested, a downregulation or stagnation at a low level was observed during the total recovery period for most genes involved in DNA repair mechanisms, which indicates that the repair mechanisms were not activated. However, the constant increase in transcription of *h2ax* during the recovery period and the increase in *rad51* expression between day 3 and 7 for plants exposed to γ_{153} suggest that DNA repair after exposure to the highest dose rate initiates later in the recovery. The effect of gamma irradiation on *rad51* gene expression observed immediately after the exposure shows that *rad51* transcription is induced in plants by the presence of chronic gamma radiation, confirming results of Van Hoeck *et al*., 2017 (80). The dose-dependent DNA repair activity of the plants aligns with the effects of the dose rates on the recovery characteristics; plants exposed to the lowest dose rate were able to initiate DNA repair already in the first three days of the recovery and at normal levels compared to the control, which corresponds to their observed growth response. While plants exposed to the highest dose rate initiated the DNA repair later and still had a stable low growth rate at the end of the recovery period. Decreases in gene expression levels at the end of the recovery period observed for the control can be explained by the age-dependency of DNA repair in plants (84).
The transcriptional results for DNA repair genes in *S. mediterranea* indicated that gamma irradiation caused either a downregulation (for *atm* and *rad51*) or stagnation (all other genes) in DNA repair activity immediately after the exposure, which remained stable throughout the first three days of the recovery (Fig. 5A-G). Additionally, during the total recovery period, DNA repair activity was stagnant or slightly increased for all applied dose rates of gamma radiation. These results indicate that the DNA repair activity was neither inhibited nor upregulated compared to the control after seven days of recovery. Furthermore, there were no differences in DNA repair activity reported that can be linked to the observed differences in recovery capacity between the three exposure levels; only the increase in *atm* expression, involved in the activation of checkpoint signaling after DSBs detection, follows a similar trend compared to the growth analyses. These results are in contrast with

previous findings of transcriptional data, reporting a persistent upregulation of genes involved in DNA damage detection and signaling (e.g. *atm*) in planaria during a recovery period of seven days upon lethal exposure to ionizing radiation (85). The dose rates applied in this study were not lethal, however, the effect of increased expression of *atm* was only observed for the lowest dose rate and not the highest ones. Additionally, Stevens *et al*., 2018 stated that DNA repair mechanisms of the neoblasts were more active during regeneration after genotoxic exposure, which could not be confirmed by these results (82). However, their conclusions were based on measurements in the stem cells, while this study analyzed the transcriptional DNA repair activity in all cell types. They also stated that the cellular responses depend on the environmental conditions (82). Furthermore, radiation is a different genotoxic agent than the MMS (a chemical substance) used in the previous study, therefore inducing slightly different cellular effects (86). Barghouth *et al*., 2019 also showed a decrease in the gene expression of genes active in the cell cycle and DNA repair (e.g. *rad51*, *pcna*) (85). This downregulation of *rad51* and *pcna*, observed after exposure to a higher lethal dose, was also present for the highest dose rate at the beginning of the recovery period in this study. However, the dose rates applied here were not lethal, so the downregulation was not present throughout the total recovery period. Another study reported that active DNA repair pathways are essential for successful migration of the neoblasts to a distal wound site, and thus, for recovery (87). As described, these findings could not be supported by our results. A possible reason for the lack of significant differences in the DNA repair activity after different levels of exposure is that the repair was only studied at the transcriptional level. Post-transcriptional signaling can induce changes in the actual activity at the protein level, which is more dynamic in its response to changes in the environment (88). Besides the absence of a link between the transcriptional levels of DNA repair activity and the growth during the recovery period, is a correlation with the mitosis activity also not observed in *S. mediterranea*.

When DNA repair mechanisms are not able to repair the damage, apoptosis can be activated as a secondary response to eliminate the cells containing the damaged DNA and can, therefore, act as an alternative for DNA repair (27, 28). Since gamma radiation induces genotoxic stress in cells, apoptosis levels are expected to rise with increasing exposure levels (64).

The protein encoded by *bag4* in *L. minor* functions to prevent apoptosis, suggesting that higher *bag4* gene expression levels are an indicator for the presence of apoptosis and the antagonization by *bag4*. The gene expression levels of *bag4* were dose-dependent (Fig. 4K). The lowest dose rate showed an increase in apoptosis in the first three days of recovery, after which it stagnated, while the increase in apoptosis for the highest dose rate initiated later, between day 3 and 7. These results correspond to observed growth rates; recovery was induced for the experimental condition with a stagnation in apoptosis, while growth was not observed for the conditions with increasing apoptotic levels. These findings confirm the previously described correlation between apoptosis and growth inhibition in *L. minor* (79). Additionally, for the highest dose rate, the apoptotic levels increase during the recovery while the DNA repair activity is low, which supports the statement that apoptosis functions as an alternative for DNA repair when the DNA damage levels are high (28).

The apoptotic activity of *S. mediterranea* was determined based on the transcriptional levels of the *bax, bcl2* and *casp3* genes (Fig. 5H-J). After seven days of recovery, the expression levels of *bax* were more upregulated for lower dose rates, indicating that activation signals for apoptosis were induced. The observations for *bax* and *bcl2* (pro- and anti-apoptotic respectively) do not match with the results observed for *casp3*. Additionally, *casp3* transcription levels show no indication of significant differences in apoptotic activity. As described above, a well-balanced interplay between apoptosis, mitosis and differentiation of the neoblasts is crucial for the remodeling and recovery of the planarians (31). But apoptosis also occurs as a response to genotoxic damage (89). It may be possible that these counteracting functions are the reason that the transcriptional analysis showed no obvious differences in apoptotic activity between the dose rates. Another possible explanation for the lack of apoptotic activity, as reported by Shiroor *et al*., 2020, states that apoptosis of the neoblasts is delayed when injury is induced immediately after radiation exposure (89). However, apoptosis was

only studied at the transcriptional level, while protein concentrations are more dynamic than transcript levels and post-transcriptional changes can alter the final responses (88). Additionally, the pathways for Caspase-3 activation are active at the protein level (30). Thus, the apoptotic activity may have changed after transcription occurred. As a result, the measured transcriptional levels for apoptotic activity do not correspond to the observed recovery capacity and mitosis levels. Furthermore, a complementary link with the DNA repair activity is also missing. These findings do not align with the previously observed interplay between mitosis, apoptosis and neoblast differentiation which controls the regeneration in planarians (31, 54).

Finally, both *L. minor* and *S. mediterranea* exhibit a dose-dependent recovery capacity after chronic exposure to high levels of gamma radiation. However, during the recovery period, no similar trends in DNA repair activity and apoptosis were observed between the two organisms. This indicates that the cellular responses to the genotoxic exposure differ between the two organisms. Indeed, the results of previous studies suggest that the DNA damage response (DDR) varies between different organisms and, by extension, between different cell types or tissues (85, 90, 91).

CONCLUSION
This study showed that the recovery capacity of both organisms depends on the applied dose rates of chronic gamma radiation. The transcriptional levels of DNA repair activity and apoptotic activity are correlated with the ability of *Lemna minor* to recover from genotoxic gamma radiation. Increases of both DNA repair and apoptosis occur right before the growth of the plants initiates, thereby functioning as an indicator for the switch from growth inhibition to recovery. Moreover, analyses in *Schmidtea mediterranea* showed a relation between the recovery capacity and the mitotic activity during the recovery period; increases in mitosis levels preceded the onset of the regeneration, thus, indicating the impending switch from growth arrest to recovery. However, the link between the recovery from genotoxic radiation and the transcriptional results on DNA repair and apoptotic activity is not as conclusive and dose-dependent in the planaria compared to the duckweed.

Further research will need to complete the analysis of the cellular mechanisms involved in the recovery of these organisms and verify the obtained results. In the next step, the signaling pathways involved in these mechanisms for recovery and their universality between the organisms can be studied.

REFERENCES

1.   Biology B. Moleculaire en Cellulaire Aspecten van Toxiciteit - Case Study: Radiotoxiciteit. 2007-2008.

2.   Koplan JP. Toxicological Profile for Ionizing Radiation. Atlanta, USA: U.S. Department of Health and Human Services - Agency for Toxic Substances and Disease Registry; 1999.

3.   Obodovskiy I. Chapter 2 - Nuclei and Nuclear Radiations. In: Obodovskiy I, editor. Radiation: Elsevier; 2019. p. 41-62.

4.   WHO. Ionizing radiation, health effects and protective measures 2020 [Available from: https://www.who.int/news-room/fact-sheets/detail/ionizing-radiation-health-effects-and-protective-measures.

5.   Willems P, Vanaudenhove T. Berekening van de jaarlijkse gemiddelde blootstelling aan ioniserende straling in België: Methodologie en Evolutie. . Belgium: FANC - Departement Gezondheid en Leefmilieu: Dienst Bescherming van de Gezondheid; 2018.

6.   Ansoborlo E, Adam-Guillermin C. 13 - Radionuclide transfer processes in the biosphere. In: Poinssot C, Geckeis H, editors. Radionuclide Behaviour in the Natural Environment: Woodhead Publishing; 2012. p. 484-513.

7.   Gerberding JL. Toxicological Profile for Cesium. Atlanta, USA: U.S. Department of Health and Human Services - Agency for Toxic Substances and Disease Registry; 2004.

8.   Nakashima J, Duong H. Radiation Physics: StatPearls Publishing, Treasure Island (FL); 2020 2020.

9.   Flakus FN. Detecting and measuring ionizing radiation - a short history. Radiation detection, IAEA Bulletin. 1981;23(4).

10.   Schmitt R. 1 - Introduction and Survey of the Electromagnetic Spectrum. Electromagnetics Explained. Burlington: Newnes; 2002. p. 1-24.

11.   Azzam EI, Jay-Gerin JP, Pain D. Ionizing radiation-induced metabolic oxidative stress and prolonged cell injury. Cancer Lett. 2012;327(1-2):48-60.

12.   Lau AH, Knakievicz T, Prá D, Erdtmann B. Freshwater planarians as novel organisms for genotoxicity testing: Analysis of chromosome aberrations. Environmental and Molecular Mutagenesis. 2007;48(6):475-82.

13.   Willers H, Dahm-Daphi J, Powell SN. Repair of radiation damage to DNA. British Journal of Cancer. 2004;90(7):1297-301.

14.   Steel GG. From targets to genes: a brief history of radiosensitivity. Phys Med Biol. 1996;41(2):205-22.

15.   Kavanagh JN, Redmond KM, Schettino G, Prise KM. DNA double strand break repair: a radiation perspective. Antioxid Redox Signal. 2013;18(18):2458-72.

16.   Chatterjee N, Walker GC. Mechanisms of DNA damage, repair, and mutagenesis. Environmental and Molecular Mutagenesis. 2017;58(5):235-63.

17.   Bleuyard J-Y, Gallego ME, Savigny F, White CI. Differing requirements for the Arabidopsis Rad51 paralogs in meiosis and DNA repair. The Plant Journal. 2004;41(4):533-45.

18.   Fell VL, Schild-Poulter C. The Ku heterodimer: Function in DNA repair and beyond. Mutation Research/Reviews in Mutation Research. 2015;763:15-29.

19.   Kobayashi W, Liu E, Ishii H, Matsunaga S, Schlögelhofer P, Kurumizaka H. Homologous pairing activities of Arabidopsis thaliana RAD51 and DMC1. J Biochem. 2019;165(3):289-95.

20.   Long DT, Raschle M, Joukov V, Walter JC. Mechanism of RAD51-Dependent DNA Interstrand Cross-Link Repair. Science. 2011;333(6038):84-7.

21.   Nicolas E, Golemis EA, Arora S. POLD1: Central mediator of DNA replication and repair, and implication in cancer and other pathologies. Gene. 2016;590(1):128-41.

22.   Sharma S, Hicks JK, Chute CL, Brennan JR, Ahn JY, Glover TW, et al. REV1 and polymerase ζ facilitate homologous recombination repair. Nucleic Acids Res. 2012;40(2):682-91.

23.   Syed A, Tainer JA. The MRE11-RAD50-NBS1 Complex Conducts the Orchestration of Damage Signaling and Outcomes to Stress in DNA Replication and Repair. Annu Rev Biochem. 2018;87:263-94.

24.   Yang Y, Gao Y, Mutter-Rottmayer L, Zlatanou A, Durando M, Ding W, et al. DNA repair factor RAD18 and DNA polymerase Polκ confer tolerance of oncogenic DNA replication stress. Journal of Cell Biology. 2017;216(10):3097-115.

25.   Peiris TH, Ramirez D, Barghouth PG, Ofoha U, Davidian D, Weckerle F, et al. Regional signals in the planarian body guide stem cell fate in the presence of genomic instability. Development. 2016;143(10):1697-709.

26.   Boehm EM, Gildenberg MS, Washington MT. The Many Roles of PCNA in Eukaryotic DNA Replication. Elsevier; 2016. p. 231-54.

27.   Siles E, Villalobos M, Jones L, Guerrero R, Eady J, Valenzuela M, et al. Apoptosis after gamma irradiation. Is it an important cell death modality? British Journal of Cancer. 1998;78(12):1594-9.

28.   UNSCEAR. Sources and effects of ionizing radiation: United Nations Scientific Committee on the Effects of Atomic Radiation 2000 Report to the General Assembly - Volume II: Effects. 2000.

29.   Doukhanina EV, Chen S, Van Der Zalm E, Godzik A, Reed J, Dickman MB. Identification and Functional Characterization of the BAG Protein Family in Arabidopsis thaliana. Journal of Biological Chemistry. 2006;281(27):18793-801.

30.   Porter AG, Jänicke RU. Emerging roles of caspase-3 in apoptosis. Cell Death & Differentiation. 1999;6(2):99-104.

31.   Pellettieri J, Fitzgerald P, Watanabe S, Mancuso J, Green DR, Sánchez Alvarado A. Cell death and tissue remodeling in planarian regeneration. Developmental Biology. 2010;338(1):76-85.

32.   Sudprasert W, Navasumrit P, Ruchirawat M. Effects of low-dose gamma radiation on DNA damage, chromosomal aberration and expression of repair genes in human blood cells. Int J Hyg Environ Health. 2006;209(6):503-11.

33.   Lemon GD, Posluszny U. Comparative Shoot Development and Evolution in the Lemnaceae. International Journal of Plant Sciences. 2000;161(5):733-48.

34.   Bednarova I, Haasova V, Mikulaskova H, Nemcova B, Strakova L, Beklova M. Comparison of the effect of platinum on producers in aquatic environment. Neuro Endocrinol Lett. 2012;33 Suppl 3:107-12.

35.   Kittiwongwattana C, Vuttipongchaikij S. Effects of nutrient media on vegetative growth of Lemna minor and Landoltia punctata during in vitro and ex vitro cultivation. Maejo International Journal of Science and Technology. 2013;7:60-9.

36.   Lemon GD, Posluszny U, Husband BC. Potential and realized rates of vegetative reproduction in Spirodela polyrhiza, Lemna minor, and Wolffia borealis. Aquatic Botany. 2001;70(1):79-87.

37.   Evans BR, Foston M, O'Neill HM, Reeves D, Rempe C, McGrath K, et al. Production of deuterated biomass by cultivation of Lemna minor (duckweed) in D(2)O. Planta. 2019;249(5):1465-75.

38.   Álvarez X, Cancela Á, Freitas V, Valero E, Sánchez Á, Acuña-Alonso C. Hydrothermal Carbonization and Pellet Production from Egeria densa and Lemna minor. Plants (Basel). 2020;9(4).

39.   Leng R, Stambolie J, Bell R. Duckweed - a potential high-protein feed resource for domestic animals and fish. FAO Livestock Research for Rural Development. 1995;7(1).

40.   Anderson KE, Lowman Z, Stomp A-M, Chang J. Duckweed as a Feed Ingredient in Laying Hen Diets and its Effect on Egg Production and Composition. International Journal of Poultry Science. 2011;10(1):4-7.

41.   Gatidou G, Oursouzidou M, Stefanatou A, Stasinakis AS. Removal mechanisms of benzotriazoles in duckweed Lemna minor wastewater treatment systems. Sci Total Environ. 2017;596-597:12-7.

42.   Walsh É, Paolacci S, Burnell G, Jansen MAK. The importance of the calcium-to-magnesium ratio for phytoremediation of dairy industry wastewater using the aquatic plant Lemna minor L. Int J Phytoremediation. 2020;22(7):694-702.

43.   Imron MF, Kurniawan SB, Soegianto A, Wahyudianto FE. Phytoremediation of methylene blue using duckweed (Lemna minor). Heliyon. 2019;5(8):e02206.

44.   Ekperusi AO, Sikoki FD, Nwachukwu EO. Application of common duckweed (Lemna minor) in phytoremediation of chemicals in the environment: State and future perspective. Chemosphere. 2019;223:285-309.

45.   Zhao H, Appenroth K, Landesman L, Salmeán AA, Lam E. Duckweed rising at Chengdu: summary of the 1st International Conference on Duckweed Application and Research. Plant Molecular Biology. 2012;78(6):627-32.

46.   OECD. Test No. 221: Lemna sp. Growth Inhibition Test2006.

47.   Van Hoeck A, Horemans N, Monsieurs P, Cao HX, Vandenhove H, Blust R. The first draft genome of the aquatic model plant Lemna minor opens the route for future stress physiology research and biotechnological applications. Biotechnology for Biofuels. 2015;8(1):188.

48.   Lázaro EM, Harrath AH, Stocchino GA, Pala M, Baguñà J, Riutort M. Schmidtea mediterraneaphylogeography: an old species surviving on a few Mediterranean islands? BMC Evolutionary Biology. 2011;11(1):274.

49.   Newmark PA, Alvarado AS. Not your father's planarian: a classic model enters the era of functional genomics. Nature Reviews Genetics. 2002;3(3):210-9.

50.   Sandmann T, Vogg MC, Owlarn S, Boutros M, Bartscherer K. The head-regeneration transcriptome of the planarian Schmidtea mediterranea. Genome Biology. 2011;12(8):R76.

51.   Karami A, Tebyanian H, Goodarzi V, Shiri S. Planarians: an In Vivo Model for Regenerative Medicine. International Journal of Stem Cells. 2015;8(2):128-33.

52.   Baguñà J. Mitosis in the intact and regenerating planarian Dugesia mediterranea n.sp. II. Mitotic studies during regeneration, and a possible mechanism of blastema formation. Journal of Experimental Zoology. 1976;195(1):65-79.

53.   Baguñà J, Saló E, Auladell C. Regeneration and patternformation in planarians. III. Evidence that neoblasts aretotipotent stem cells and the source of blastema cells. Development. 1989;107:77-86.

54.   Almuedo-Castillo M, Crespo-Yanez X, Seebeck F, Bartscherer K, Salò E, Adell T. JNK controls the onset of mitosis in planarian stem cells and triggers apoptotic cell death required for regeneration and remodeling. PLoS Genet. 2014;10(6):e1004400-e.

55.   Oviedo NJ, Newmark PA, Sánchez Alvarado A. Allometric scaling and proportion regulation in the freshwater planarian Schmidtea mediterranea. Developmental Dynamics. 2003;226(2):326-33.

56.   Plusquin M, DeGheselle O, Cuypers A, Geerdens E, Van Roten A, Artois T, et al. Reference genes for qPCR assays in toxic metal and salinity stress in two flatworm model organisms. Ecotoxicology. 2012;21(2):475-84.

57.   Ofoegbu PU, Campos D, Soares A, Pestana JLT. Combined effects of NaCl and fluoxetine on the freshwater planarian, Schmidtea mediterranea (Platyhelminthes: Dugesiidae). Environ Sci Pollut Res Int. 2019;26(11):11326-35.

58.   Tran TA, Hesler M, Moriones OH, Jimeno-Romero A, Fischer B, Bastús NG, et al. Assessment of iron oxide nanoparticle ecotoxicity on regeneration and homeostasis in the replacement model system Schmidtea mediterranea. Altex. 2019;36(4):583-96.

59.   Stevens AS, Pirotte N, Plusquin M, Willems M, Neyens T, Artois T, et al. Toxicity profiles and solvent-toxicant interference in the planarian Schmidtea mediterranea after dimethylsulfoxide (DMSO) exposure. J Appl Toxicol. 2015;35(3):319-26.

60.   Robb SM, Gotting K, Ross E, Sánchez Alvarado A. SmedGD 2.0: The Schmidtea mediterranea genome database. Genesis. 2015;53(8):535-46.

61.   Grohme MA, Schloissnig S, Rozanski A, Pippel M, Young GR, Winkler S, et al. The genome of Schmidtea mediterranea and the evolution of core cellular mechanisms. Nature. 2018;554(7690):56-61.

62.   Gaillochet C, Lohmann JU. The never-ending story: from pluripotency to plant developmental plasticity. Development (Cambridge, England). 2015;142(13):2237-49.

63.   Wagner DE, Wang IE, Reddien PW. Clonogenic neoblasts are pluripotent adult stem cells that underlie planarian regeneration. Science. 2011;332(6031):811-6.

64.   Adam-Guillermin C, Hertal-Aas T, Oughton D, Blanchard L, Alonzo F, Armant O, et al. Radiosensitivity and transgenerational effects in non-human species. Ann ICRP. 2018;47(3-4):327-41.

65.   Mujoo K, Butler EB, Pandita RK, Hunt CR, Pandita TK. Pluripotent Stem Cells and DNA Damage Response to Ionizing Radiations. Radiation Research. 2016;186(1):17-26.

66.   Wyles S, Brandt E, Nelson T. Stem Cells: The Pursuit of Genomic Stability. International Journal of Molecular Sciences. 2014;15(11):20948-67.

67.   UNSCEAR. Sources and effects of ionizing radiation: United Nations Scientific Committee on the Effects of Atomic Radiation 1996 Report to the General Assembly. 1996.

68.   Murray JM, Carr AM. Integrating DNA damage repair with the cell cycle. Curr Opin Cell Biol. 2018;52:120-5.

69.   Pietenpol JA, Stewart ZA. Cell cycle checkpoint signaling: cell cycle arrest versus apoptosis. Toxicology. 2002;181-182:475-81.

70.   Friesner JD, Liu B, Culligan K, Britt AB. Ionizing Radiation–dependent γ-H2AX Focus Formation Requires Ataxia Telangiectasia Mutated and Ataxia Telangiectasia Mutated and Rad3-related. Molecular Biology of the Cell. 2005;16(5):2566-76.

71.   Van Hoeck A, Horemans N, Van Hees M, Nauts R, Knapen D, Vandenhove H, et al. Characterizing dose response relationships: Chronic gamma radiation in Lemna minor induces oxidative stress and altered polyploidy level. Journal of Environmental Radioactivity. 2015;150:195-202.

72.   Baguñà J. Estudios citotaxonómicos, ecológicos e histofisiología dela regulación morfogenética durante el crecimiento y la regeneraciónen la raza asexuada de la planaria Dugesia mediterranea. PhD thesis. Barcelona: University of Barcelona; 1973.

73.   Benazzi M, Baguná J, Ballester R, Puccinelli I, Papa RD. Further Contribution to the Taxonomy of the «Dugesia Lugubris-Polychroa Group» with Description of Dugesia Mediterranea N.SP. (Tricladida, Paludicola). Bolletino di zoologia. 1975;42(1):81-9.

74.   Bustin SA, Benes V, Garson JA, Hellemans J, Huggett J, Kubista M, et al. The MIQE Guidelines: Minimum Information for Publication of Quantitative Real-Time PCR Experiments. Clinical Chemistry. 2009;55(4):611-22.

75.   Bustin SA, Beaulieu J-F, Huggett J, Jaggi R, Kibenge FS, Olsvik PA, et al. MIQE précis: Practical implementation of minimum standard guidelines for fluorescence-based quantitative real-time PCR experiments. BMC Molecular Biology. 2010;11(1):74.

76.   Pirotte N, Stevens A-S, Fraguas S, Plusquin M, Van Roten A, Van Belleghem F, et al. Reactive Oxygen Species in Planarian Regeneration: An Upstream Necessity for Correct Patterning and Brain Formation. Oxidative Medicine and Cellular Longevity. 2015;2015:1-19.

77.   Livak KJ, Schmittgen TD. Analysis of Relative Gene Expression Data Using Real-Time Quantitative PCR and the 2−ΔΔCT Method. Methods. 2001;25(4):402-8.

78.   Plusquin M, Stevens A-S, Van-Belleghem F, Degheselle O, Van-Roten A, Vroonen J, et al. Physiological and molecular characterisation of cadmium stress in Schmidtea mediterranea. The International Journal of Developmental Biology. 2012;56(1-2-3):183-91.

79.   Xie L, Solhaug KA, Song Y, Brede DA, Lind OC, Salbu B, et al. Modes of action and adverse effects of gamma radiation in an aquatic macrophyte Lemna minor. Sci Total Environ. 2019;680:23-34.

80.   Van Hoeck A, Horemans N, Nauts R, Van Hees M, Vandenhove H, Blust R. Lemna minor plants chronically exposed to ionising radiation: RNA-seq analysis indicates a dose rate dependent shift from acclimation to survival strategies. Plant Science. 2017;257:84-95.

81.   Gavlik A, Szymczak RK. Retardation of Planaria Regeneration by Ultraviolet Radiation. Bios. 2003;74(4):118-23.

82.   Stevens A-S, Wouters A, Ploem J-P, Pirotte N, Van Roten A, Willems M, et al. Planarians Customize Their Stem Cell Responses Following Genotoxic Stress as a Function of Exposure Time and Regenerative State. Toxicological Sciences. 2018;162(1):251-63.

83.   Wouters A, Ploem JP, Langie SAS, Artois T, Aboobaker A, Smeets K. Regenerative responses following DNA damage - β-catenin mediates head regrowth in the planarian Schmidtea mediterranea. J Cell Sci. 2020;133(8).

84.   Golubov A, Yao Y, Maheshwari P, Bilichak A, Boyko A, Belzile F, et al. Microsatellite instability in Arabidopsis increases with plant development. Plant Physiol. 2010;154(3):1415-27.

85.   Barghouth PG, Thiruvalluvan M, LeGro M, Oviedo NJ. DNA damage and tissue repair: What we can learn from planaria. Semin Cell Dev Biol. 2019;87:145-59.

86.   Lackinger D. Effect of ultraviolet light, methyl methanesulfonate and ionizing radiation on the genotoxic response and apoptosis of mouse fibroblasts lacking c-Fos, p53 or both. Mutagenesis. 2001;16(3):233-41.
87.   Sahu S, Sridhar D, Abnave P, Kosaka N, Dattani A, Thompson JM, et al. Ongoing repair of migration-coupled DNA damage allows planarian adult stem cells to reach wound sites. eLife. 2021;10.
88.   Vogel C, Marcotte EM. Insights into the regulation of protein abundance from proteomic and transcriptomic analyses. Nature Reviews Genetics. 2012;13(4):227-32.
89.   Shiroor DA, Bohr TE, Adler CE. Injury Delays Stem Cell Apoptosis after Radiation in Planarians. Current Biology. 2020;30(11):2166-74.e3.
90.   Lans H, Vermeulen W. Tissue specific response to DNA damage: C. elegans as role model. DNA Repair. 2015;32:141-8.
91.   Nisa M-U, Huang Y, Benhamed M, Raynaud C. The Plant DNA Damage Response: Signaling Pathways Leading to Growth Inhibition and Putative Role in Response to Stress Conditions. Frontiers in Plant Science. 2019;10.

SUPPLEMENTARY MATERIAL

Table S1 – Overview of the experimental set-up of chronic gamma radiation exposure.

Name exposure	Distance to source (cm)	Dose rate (mGy/h)	Total dose after 7 days (mGy)
Lemna minor			
γ_{68}	106	68	12398 ± 305
γ_{116}	77	116	21146 ± 519
γ_{153}	69	153	27839 ± 684
Schmidtea mediterranea			
γ_{18}	198	18	3340 ± 96
γ_{29}	158	29	5241 ± 150
γ_{83}	101	83	15007 ± 430

Table S2 – qPCR specifications for *L. minor* based on the MIQE guidelines.

Sample/Template	Details
Sample source	*Lemna minor* plants (30-50 mg per sample)
Sample preservation	Snap frozen in liquid N_2, storage at -80°C
Extraction method	Shredding with 3 chrome steel beads (d=2.3 mm) for 3.5 min at 30 Hz & RNeasy Plant Mini Kit (QIAGEN)
RNA concentration & purity measurement	NanoDrop ND-1000 spectrophotometry (Isogen)
RNA preservation	Snap frozen in liquid N_2, storage at -80°C
RNA: DNase treatment	TURBO DNA-free kit (Invitrogen)
cDNA synthesis	TaKaRa PrimeScript RT Reagent kit (TaKaRa Bio Inc.)
RNA input for cDNA synthesis	1000 ng in 13 µL
cDNA preservation	Storage at -20°C

Primer design/manufacturing/testing	Details
Method based on FASTA file containing a 'transdecoder' of *L. minor* transcripts, based on previous work of the research group at SCK CEN	FASTA sequence of the gene of interest was analyzed with the Primer-BLAST function of NCBI, using the "transdecoder" file as custom database
	10 random primer pairs designed
	PCR product size: 70 to 150 bp
	Testing primer pairs fit for qPCR with the Oligo Analysis Tool of Eurofins Genomics
Method based on the genome of *Arabidopsis thaliana*, using The Arabidopsis Information Resource (TAIR) to obtain the FASTA sequence of the gene of interest by using its BLAST function	FASTA sequence of the gene of interest was analyzed with the Primer-BLAST function of the National Center for Biotechnology Information (NCBI), using the "transdecoder" file as custom database, providing 10 random primer pairs for the corresponding gene
	PCR product size: 70 to 150 bp
	Testing primer pairs fit for qPCR with the Oligo Analysis Tool of Eurofins Genomics
Manufacturer primers	Eurogentec (Seraing, Belgium)
Primer purification method	SePOP
Primers delivered	100 µM diluted in MilliQ water
Primers diluted	10x diluted in nuclease-free water (10 µM)
Primer efficiency testing	4x dilution curve of pooled sample (1:1 1:4 1:16 1:64 1:256 1:1024) and 2 NTC's
Efficiency calculation	Based on slope of logarithm of the dilution curve: between 90 - 118%: included

Primer sequences	Details		
DNA repair genes	Function	Forward primer	Revere primer
ATM serine/threonine kinase *(atm)*	Activating checkpoint signaling when DSBs are detected	GATTCCACGGCTACTGGCAT	CGCAATCACCAGCAAGACAC
ATR serine/threonine kinase *(atr)*	Activating checkpoint signaling when DNA damage is detected	CCCATGTTCCAGCCTGTCTT	CCACTATGTGCCCCACCATT
H2A histone family member X *(h2ax)*	Activating cell cycle arrest for DSB repair	ACGACGAGGAACTCAGCAAG	ACTCCTGAGAAGCAGATCCGA
MRE11 homolog, double strand break repair nuclease *(mre11)*	Involved in DSB repair	CTTCCGAGTCTCGTCAATCCC	AATGTCATCTCCTCCTGAGCG
Proliferating cell nuclear antigen *(pcna)*	Involved in NER and TLS	CTACCATCCAGATGCCGTCC	ATCGTTCGTACCTGTGTCGC
DNA polymerase delta 1 *(pold1)*	Involved in DNA replication, BER, NER, TLS, MMR and DSB repair	TCTCCTTCGACACAGAGAGAG	CTATTCCAAGTGACTCGGCT
RAD18 E3 ubiquitin protein ligase *(rad18)*	Involved in DSB repair, ICL repair and TLS	GCTTTGGCAGACCGAGAGAT	GGGCTAGAACCCTTTCCGAC
RAD50 double strand break repair protein *(rad50)*	Involved in HR for DSB repair	AACTTGCCCGCGAGATTGAA	ACCGAAATTGTGCCCTGAAAC
RAD51 recombinase *(rad51)*	Involved in HR for DSB repair and ICL repair	GACGGATCGGCCATGTTCA	CGACGCTATCACCTTGCAGA
REV1 DNA directed polymerase *(rev1)*	Involved in DSB repair and TLS	ATTGCATGAGCACTGTCCGA	AGCACTAGCAGAGCAACCAG
Apoptosis genes			
Bcl-2 associated athanogene 4 *(bag4)*	Anti-apoptotic regulator	AAGGCGGTGAAACTTTGCTC	ATTCATGTGCCCCTTGTGCT
Reference genes			
BSL2 serine/threonine-protein phosphatase *(bsl2)*	Housekeeping gene	GCGCCGATCCTAGATTTGAA	CAGGCCCATCCTCCTTCTTC
Cytochrome P450 71A25 *(cyp71a25)*	Housekeeping gene	TTGAGCTTGCTCTTGCTGGT	TCCTGCGAATGGTAAAGCCC
Gamma-tubulin complex component 3 *(gcp3)*	Housekeeping gene	TCGTCAGCCAGCCAGTAAAG	AGTCTCCCTGTCCGAGAAGA
Mitogen-activated protein kinase kinase 1 *(map2k1)*	Housekeeping gene	TTGGATCATGAGGGGAAGGAG	CGTCCTGAAAGACGCCACAA
SBT3.3 subtilisin-like protease *(sbt3.3)*	Housekeeping gene	GAGACGGGGCAAGAGTTCAA	CATCCACCGGCTAACCCATT
Tubulin beta-5 chain *(tubb5)*	Housekeeping gene	TTCGTCCGGATAGCTTCGTG	GCCATTTTCGGATTCCTCGC

Real-time qPCR	Details
cDNA sample used in qPCR	10x diluted, 3.75 µL input
Master mix	Total volume: 11.25 µL:
	7.5 µL Fast SYBR Green Master Mix (Applied Biosystems)
	0.45 µL Forward primer (10µM)
	0.45 µL Reverse primer (10µM)
	2.85 µL nuclease-free water
cDNA & master mix pipetting	Pipetted by QIAgility pipetting robot (QIAGEN) in Rotor-Disc 100 with 100 wells (QIAGEN)
qPCR instrument	Rotor-Gene Q (QIAGEN)
qPCR thermal cycling	45 cycles and melt curve

Data analysis	Details
qPCR analysis program	Rotor-Gene Q Software (QIAGEN)
Cq value determination	Log scale with Dynamic Tube on; threshold: 0.1
Selection reference genes (normalization)	geNorm analysis in qbase+ software (Biogazelle): best combination: *sbt3.3, tubb5, gcp3* and *map2k1*
Relative gene expression calculation	$2^{-\Delta\Delta Ct}$ method & normalization factor of the reference genes
Biological replicates	6 per dose rate and sampling moment

Table S3 – qPCR specifications for *S. mediterranea* based on the MIQE guidelines.

Sample/Template	Details		
Sample source	*Schmidtea mediterranea* heads or tails (3 organisms per sample)		
Sample preservation	Snap frozen in liquid N_2, storage at -80°C		
Extraction method	Lysis using an RLT lysis buffer containing 1% beta-mercaptoethanol & Phenol/Chloroform extraction protocol (Pirotte *et al*. 2015)		
RNA concentration & purity measurement	NanoDrop ND-1000 spectrophotometry (Isogen)		
RNA preservation	Snap frozen in liquid N_2, storage at -80°C		
RNA: DNase treatment	TURBO DNA-free kit (Invitrogen)		
cDNA synthesis	TaKaRa PrimeScript RT Reagent kit (TaKaRa Bio Inc.)		
RNA input for cDNA synthesis	500 ng in 13 µL		
cDNA preservation	Storage at -20°C		
Primer design/manufacturing/testing	**Details**		
Method performing FASTA sequence search of the gene of interest in multiple databases: NCBI, SmedGD, PlanMine, PlanNet	FASTA sequence of the gene of interest was analyzed with the Primer-BLAST function NCBI, using the full-length transcript		
	10 random primer pairs designed		
	PCR product size: 70 to 200 bp		
	Testing primer pairs fit for qPCR with the Oligo Analysis Tool of Eurofins Genomics		
Manufacturer primers	Biolegio B.V. (Nijmegen, The Netherlands)		
Primer purification method	/		
Primers delivered	Lyophilized		
Primer dissolution	In TE-buffer (1mM EDTA, 10 mM Tris HCl pH 8.0) until concentration of 100 µM		
Primers diluted	10x diluted in nuclease-free water (10 µM)		
Primer efficiency testing	3x dilution curve of pooled sample (1:1 1:3 1:9 1:27 1:81) and 2 NTC's		
Efficiency calculation	Based on slope of logarithm of the dilution curve: between 91 - 116%: included		
Primer sequences	**Details**		
DNA repair genes	**Function**	**Forward primer**	**Reverse primer**
ATM serine/threonine kinase *(atm)*	Activating checkpoint signaling when DSBs are detected	AAACTGATGCCGACTCAAGAA	ATGGATCGTGAAGCAAAACC
Ku80 protein encoded by XRCC5 gene *(ku80)*	Involved in NHEJ for DSB repair	CTGGTCGGTTACACGAAGGT	CCGATTTGAATGATTGTGGT
Proliferating cell nuclear antigen *(pcna)*	Involved in NER and TLS	TCTTCTCAAGTATCTCTGTCGTTG	CTCGTCGTCTTCGATTTTAGG
DNA polymerase delta 1 *(pold1)*	Involved in DNA replication, BER, NER, TLS, MMR and DSB repair	TTGTGGACCGAATGTCAGCG	TCGGGCAATCTCGGTTAGAA
RAD50 double strand break repair protein *(rad50)*	Involved in HR for DSB repair	AGACACGTTGCAAATTCGGC	CGAAACTCCAACGAATCAATCTGT
RAD51 recombinase *(rad51)*	Involved in HR for DSB repair and ICL repair	GTTTACCGCAGATCCCAAGA	TCACCTCGACCTTTCCTCAA
REV1 DNA directed polymerase *(rev1)*	Involved in DSB repair and TLS	AAACGGAATGCATCTTGGCA	TCGCAACTTCCAACTTCGAT
Apoptosis genes			
BCL2-associated X protein *(bax)*	Pro-apoptotic regulator	CAAGTCGGCTTTTAATGATTTCTC	AAACAGGTATACGATTGCGTTCCA
B-cell lymphoma 2 *(bcl2)*	Anti-apoptotic regulator	GGGTCAGAGAAAATGGAGGA	TATCCCCAGGGCCACTTT
Caspase 3 *(casp3)*	Involved in execution of apoptosis	ATTCAAGCCTGTCGTGGTG	CAGCTTCAATTGGAATCTTTTCT
Reference genes			
Beta-actine *(b-act)*	Housekeeping gene	AGAACAGCTTCAGCCTCGTCA	TGGAATAGTGCTTCTGGGCAT
Cystatin-like *(cys)*	Housekeeping gene	AACTCCATGGCTAGAACCGAA	CCGTCGGGTAATCCAAGTACA
Glyceraldehyde-3-phosphate dehydrogenase *(gapdh)*	Housekeeping gene	GCAAAACATTATTCCGGCTTC	GCACTGGAACTCTAAAGGCCA
GM2 ganglioside activator pseudogene *(gm2ap)*	Housekeeping gene	CCGTCAGATTAAAGCTCGGTT	TTTCGGACATTCGTTACCCAT
Peptidylprolyl isomerase A *(ppia)*	Housekeeping gene	GCAAATGCAGGTCCAAATACA	ATGCCTTCAGCAACTTCTCC
Ribosomal protein L13a *(rpl13a)*	Housekeeping gene	AGGTGTCCCAGCTCCTTATGA	GGCCCAATTGACAGAATTTTC
Real-time qPCR	**Details**		
cDNA sample used in qPCR	5x diluted, 2.5 µL input per well		
Master mix	Total volume per well: 7.5 µL:		
	5 µL Fast SYBR Green Master Mix (Applied Biosystems)		
	0.3 µL Forward primer (10µM)		
	0.3 µL Reverse primer (10µM)		
	1.9 µL nuclease-free water		
cDNA & master mix pipetting	Pipetted by hand using automatic multichannel pipettes (Viaflo, Integra) in 384-well plates (Thermo Fisher Scientific)		
qPCR instrument	QuantStudio 5 Real-Time PCR System, 384-well format (Applied Biosystems)		
qPCR thermal cycling	40 cycles and melt curve		
Data analysis	**Details**		
qPCR analysis program	Thermo Fisher Connect cloud software (Thermo Fisher Scientific)		
Cq value determination	Log scale; threshold: 0.3		
Selection reference genes (normalization)	geNorm analysis in qbase+ software (Biogazelle). Best combination: *b-act* and *cys*		
Relative gene expression calculation	$2^{-\Delta\Delta Ct}$ method & normalization factor of the reference genes		
Biological replicates	3 to 6 per dose rate and sampling moment		

Method S1 – *Staining for mitotic index*

First samples were fixed for 1 hour at 4°C with fixing solution containing 0.03% glutaraldehyde and 0.1 M cacodylate. Next, they were incubated overnight at 4°C in fresh fixing solution. Then, the samples were dehydrated with an ethanol series (30% for 10 min, 50% for 10 min, 70% overnight (4°C), 90% for 30 min, 90% for 30 min, 100% for 60 min, 100% for 60 min and 100% for 120 min). Subsequently, clearing of the samples was performed by incubating the samples in 1:1 ethanol/xylene for 60 min, followed by incubation in 100% xylene overnight and two times 120 min in fresh xylene. Then, samples were embedded and solidified in paraffin, and 5 μm sections were made. Before staining was executed, deparaffinization and rehydration of the sections was performed with the following washing steps (all with a duration of 3 min): 100% xylene, 100% xylene, 1:1 xylene/ethanol, 100% ethanol, 100% ethanol, 95% ethanol, 70% ethanol and 50% ethanol. Slides were kept in dH_2O until the next step of covering the slide with 1M HCl at 60°C for 10 to 20 min. For toluidine blue staining, two droplets (0.1%) were added on each sample and incubated for 1 min at room temperature (RT), followed by 3 washes in dH_2O. Mounting with 50% glycerol and a wash step series of ethanol (95%, 95%, 100%, 100%) and xylene (2x) finished with DPX mounting was tested. Staining with Schiff's reagent was performed by incubating the slides 30-90 min at RT in a dark Falcon tube with Schiff's reagent.

Method S2 – *Alkaline comet assay, modifications to protocol as described by Xie et al., 2019 (79)*

Both organisms were chopped for 30 sec in 250 μL of PBS/EDTA extraction buffer. Gels of 10 μL of the agarose sample were molded in triplicate on the coated slide. These steps were repeated for another three samples on the same slide (12-gel slide format). After 5 min of incubation at room temperature (RT), planarian slides were incubated for 2h at 4°C in lysis buffer with pH=10 (1% Triton X-100, 10% DMSO, 2.5 M NaCl, 0.1 M Na_2EDTA, 10 mM Tris-HCl) followed by denaturation for 15 min at 4°C in the electrophoresis buffer, while *L. minor* samples were immediately immersed in the electrophoresis buffer. Next, electrophoresis was activated for 10 min at 12V. After electrophoresis, slides were neutralized by incubation once in dH_2O for 1 min and twice in PBS (pH=7) for 5 min. Subsequently, the gels were fixed by incubation in 70% ethanol for 15 min and in 95% ethanol for 15 min. The slides were dried overnight at RT. Finally, the staining of the nuclei was performed with 1:10.000 SYBR Gold Nuclear Acid Gel Stain (Invitrogen, Thermo Fisher Scientific, Waltham, Mass, USA) for 40 min in the dark. Slides were washed three times in dH_2O and dried before visualization.
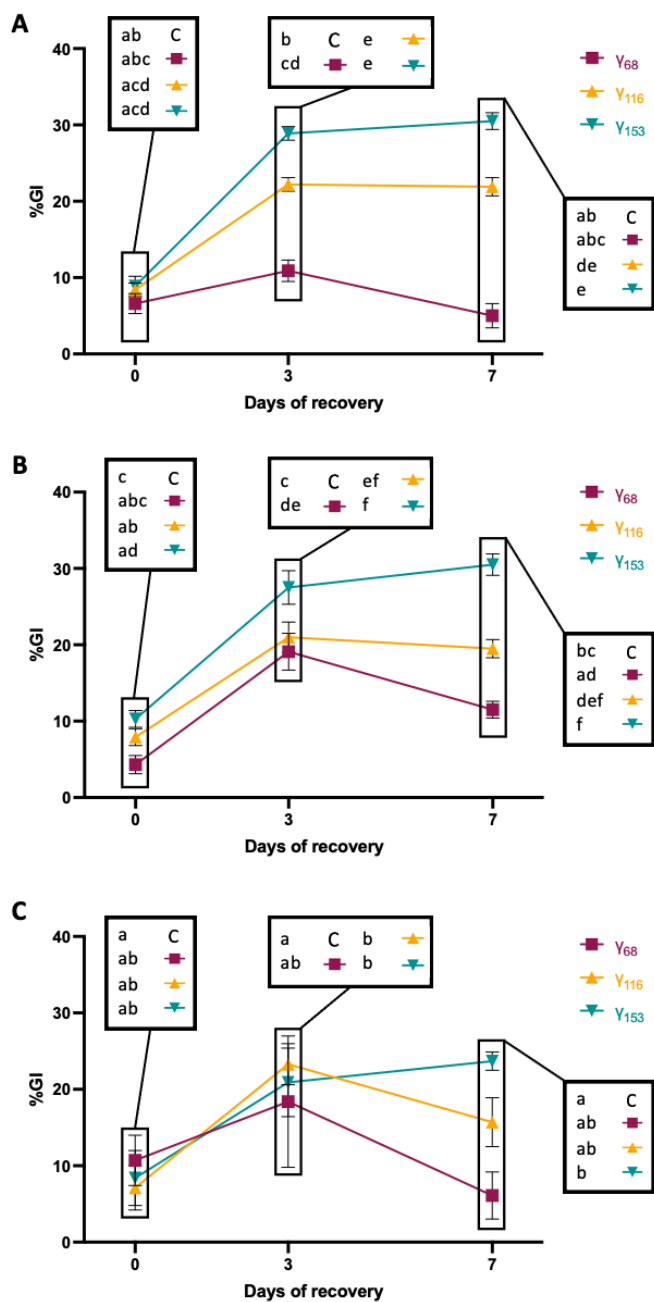
Fig. S1 – The percentage of growth inhibition (%GI) of *L. minor* compared to 0% growth inhibition for the control C. The growth inhibition was determined at day 0, 3 and 7 of the recovery after seven days of exposure to three different dose rates of γ-radiation ($γ_{68}$, $γ_{116}$ and $γ_{153}$). Calculations are based on (A) the total frond area, (B) the number of fronds and (C) fresh weight.
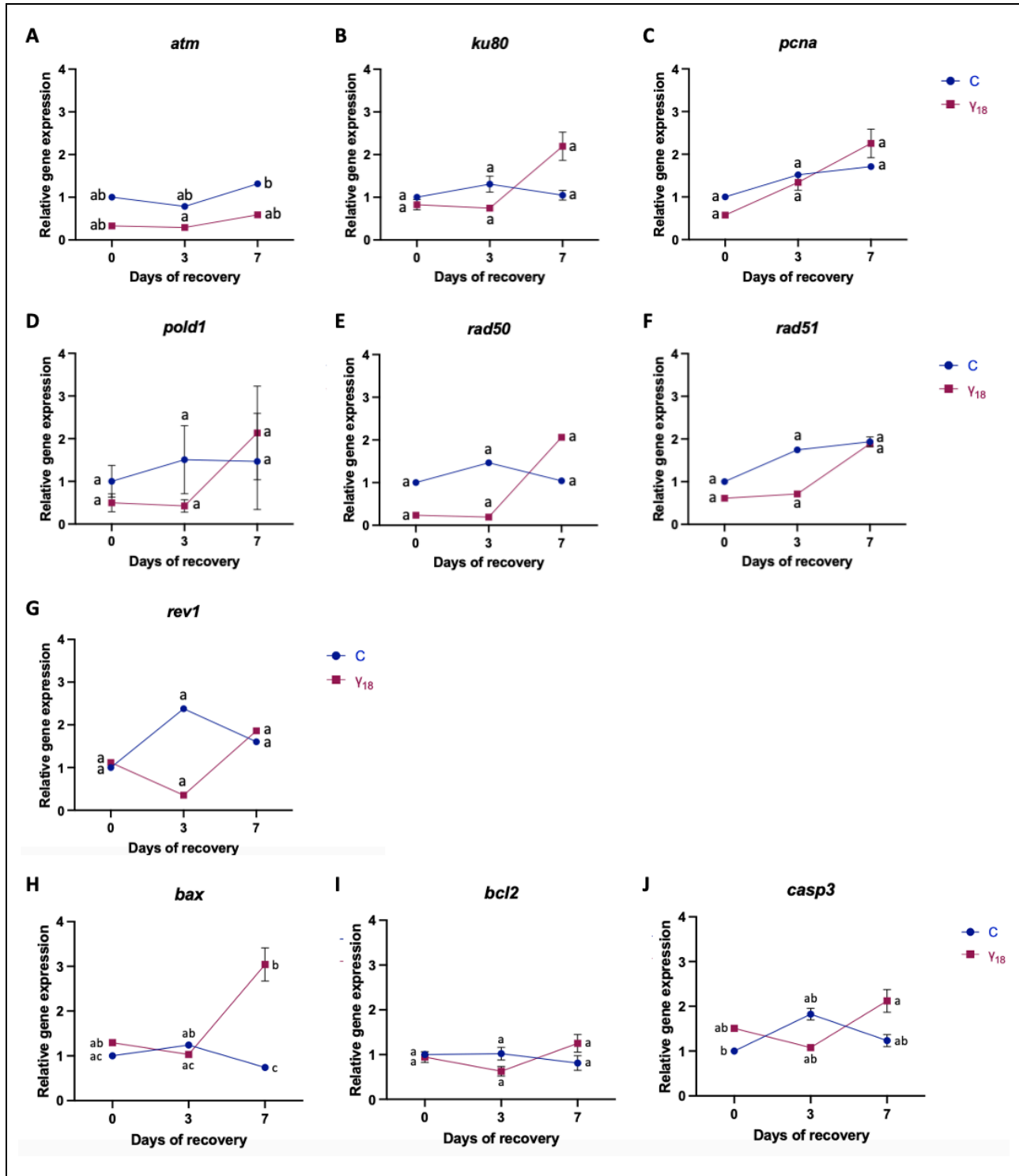
Fig. S2 – Relative gene expression levels of the heads of *S. mediterranea* determined at day 0, 3 and 7 of the recovery after seven days of exposure to 18 mGy/h of γ-radiation (γ18), compared to unexposed controls C. The genes are involved in (A-G) DNA repair pathways and (H-J) apoptotic regulation.
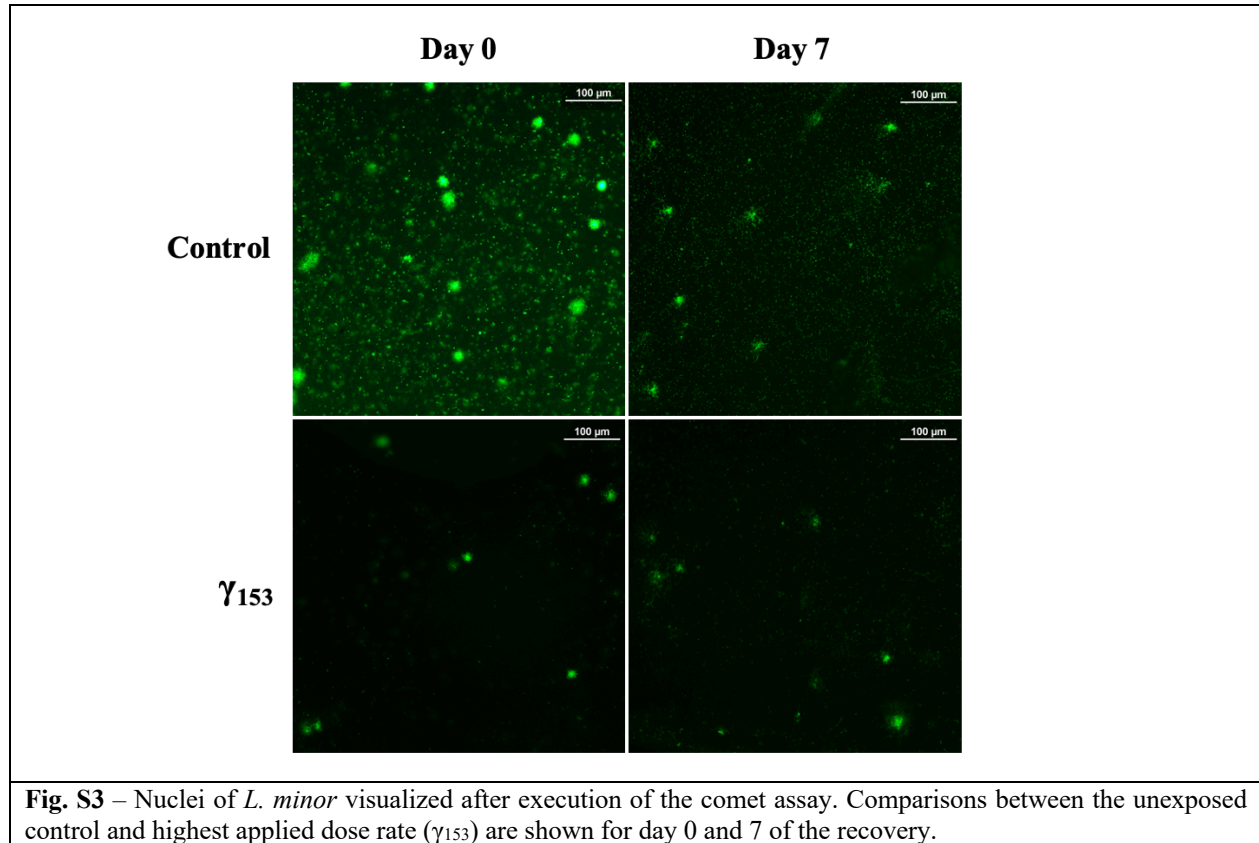
Fig. S3 – Nuclei of *L. minor* visualized after execution of the comet assay. Comparisons between the unexposed control and highest applied dose rate (γ_{153}) are shown for day 0 and 7 of the recovery.

Fig. S4 – Nuclei of *S. mediterranea* heads (H) and tails (T) visualized after execution of the comet assay. Comparisons between the unexposed control and highest applied dose rate (γ83) are shown for day 0 and 7 of the recovery.